SUMMER 2023
electronics-cooling.com

electronics COOLING

FEATURED IN THIS EDITION

16 ADVANCED COOLING SYSTEM FOR MODULAR ELECTRONICS THERMAL MANAGEMENT

22 RAPID AND ACCURATE ANALYTICAL MODEL FOR PREDICTING AXIAL FAN PERFORMANCE IN ELECTRONICS COOLING

27 A COMPARATIVE SUMMARY OF DATA CENTER COOLING STRATEGIES

9 SUMMARY OF SEMI-THERM 2023 CONFERENCE

12 CALCULATION CORNER
CALCULATING THERMAL DESIGN POWER FOR MOBILE CONSUMER ELECTRONICS – PART 2

© Copyright 2023 Electronics Cooling

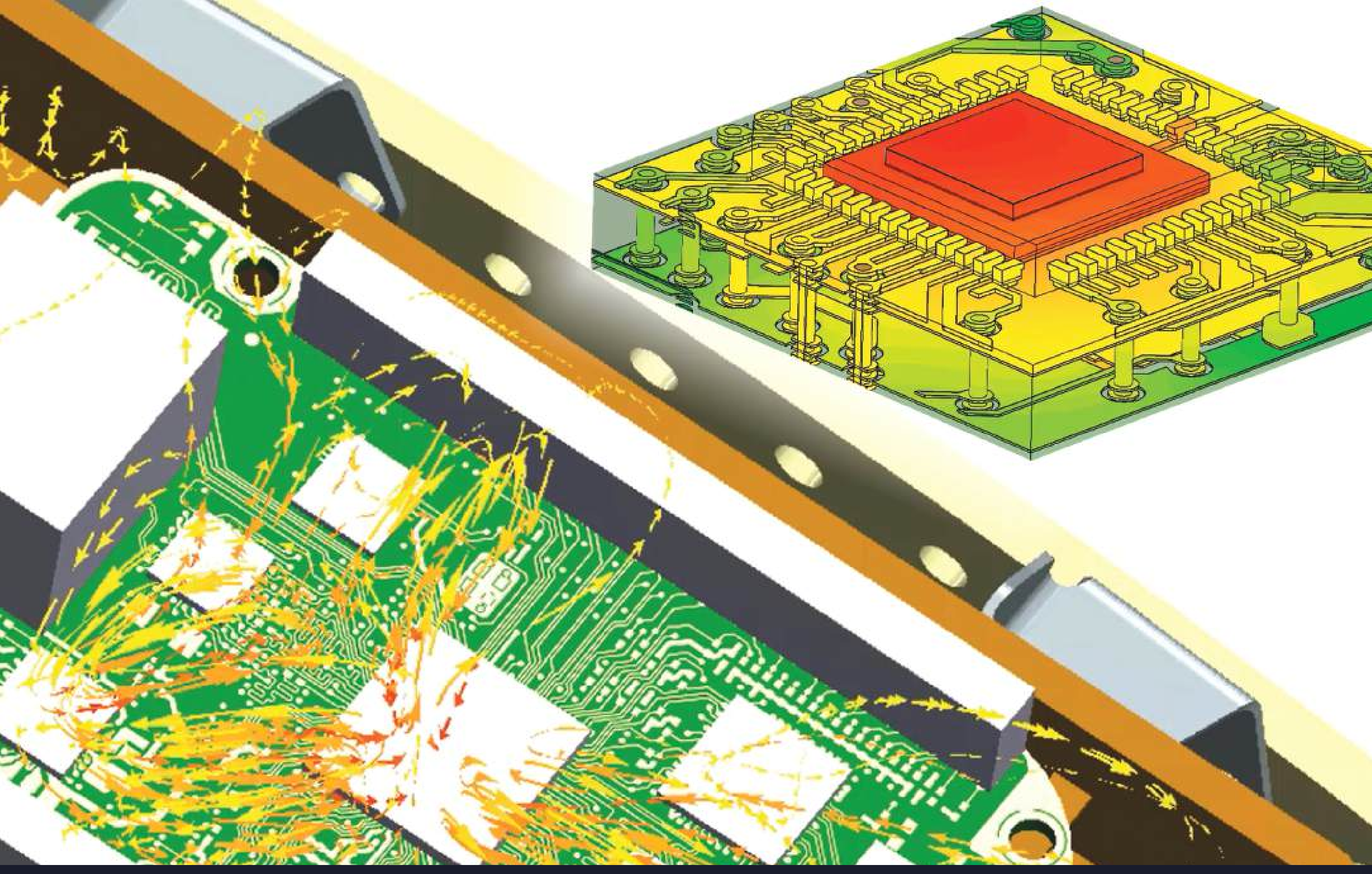

Accelerate thermal, thermo-mechanical and electro-thermal workflows

Leverage efficient CFD and FEA workflows for shorter, robust thermal and thermo-mechanical analysis. Underpin simulation accuracy with thermal measurement for characterization, calibration to reliability assessment. Incorporate EDA and MCAD data complexity efficiently into simulation. Enable PCB electro-thermal modeling using power integrity co-simulation. Realize the advantage of novel reduced order thermal model generation from full 3D analysis to improve accuracy in circuit or system modeling.

Simcenter provides simulation and test solutions to support you in developing a thermal digital twin. The portfolio includes a range of leading electronics cooling software , CAD-embedded CFD simulation options, and multi-physics analysis tools to support a wider range of user skill and experience demographic from analyst to designer. Learn how Siemens Digital Industries Software can help you achieve digital transformation goals.

www.siemens.com/simcenter

SIEMENS

CONTENTS

4 **INTERESTING TIMES**
Ross Wilcoxon

6 **TECHNICAL EDITORS SPOTLIGHT**

7 **COOLING EVENTS**
News of Upcoming 2023 Thermal Management Events

9 **SUMMARY OF SEMI-THERM 2023 CONFERENCE**
Marcelo del Valle, Lieven Vervecken and Alex Ockfen

12 **CALCULATION CORNER**
Calculating Thermal Design Power for Mobile Consumer Electronics – Part 2
Alex Ockfen

16 **ADVANCED COOLING SYSTEM FOR MODULAR ELECTRONICS THERMAL MANAGEMENT**
Sai Kiran Hota, Kuan-Lin Lee, Greg Hoeschele, Srujan Rokkam

22 **RAPID AND ACCURATE ANALYTICAL MODEL FOR PREDICTING AXIAL FAN PERFORMANCE IN ELECTRONICS COOLING**
Wenguang Zhao, Sahan Wasala, and Tim Persoons

27 **A COMPARATIVE SUMMARY OF DATA CENTER COOLING STRATEGIES**
Tim Shedd, Emily B. Clark

34 **INDEX OF ADVERTISERS**

PUBLISHED BY
Lectrix
716 Dekalb Pike, #351
Blue Bell, PA 19422
Phone: +1 484-688-0300; Fax:+1 484-688-0303
info@lectrixgroup.com
lectrixgroup.com

CHIEF EXECUTIVE OFFICER
Graham Kilshaw | graham@lectrixgroup.com

GENERAL MANAGER
Grant Hultgren | grant@lectrixgroup.com

DIRECTOR OF MEDIA & EVENTS
Katherine Struve | katherine@lectrixgroup.com

DIRECTOR OF BUSINESS DEVELOPMENT
Ashlee Zapata-McCants | ashlee@lectrixgroup.com

CREATIVE DIRECTOR
Kate Teti | kate@lectrixgroup.com

DIRECTOR OF OPERATIONS
Stephanie Curry | stephanie@lectrixgroup.com

TRAFFIC COORDINATOR
Mackenzie Mann | mackenzie@lectrixgroup.com

EDITORIAL BOARD

Victor Chiriac, PhD, ASME Fellow
Co-founder and Managing Partner
Global Cooling Technology Group
vchiriac@gctg-llc.com

Genevieve Martin
R&D Manager, Thermal & Mechanics Competence
Signify
genevieve.martin@signify.com

Alex Ockfen, P.E.
Manager, Thermal & Mechanical Simulation
Meta
alex.ockfen@fb.com

Ross Wilcoxon, Ph.D.
Senior Technical Fellow
Collins Aerospace
ross.wilcoxon@collins.com

►SUBSCRIPTIONS ONLINE
at electronics-cooling.com

For subscription changes email
info@electronics-cooling.com

All rights reserved. No part of this publication may be reproduced or transmitted in any form or by any means, electronic, mechanical, photocopying, recording or otherwise, or stored in a retrieval system of any nature, without the prior written permission of the publishers (except in accordance with the Copyright Designs and Patents Act 1988).

The opinions expressed in the articles, letters and other contributions included in this publication are those of the authors and the publication of such articles, letters or other contributions does not necessarily imply that such opinions are those of the publisher. In addition, the publishers cannot accept any responsibility for any legal or other consequences which may arise directly or indirectly as a result of the use or adaptation of any of the material or information in this publication.

ElectronicsCooling is a trademark of Mentor Graphics Corporation and its use is licensed to Lectrix. Lectrix is solely responsible for all content published, linked to, or otherwise presented in conjunction with the ElectronicsCooling trademark.

Lectrix®, Electronics Cooling®—The **2023 Summer Edition** is distributed digitally at no charge to engineers and managers engaged in the application, selection, design, test, specification or procurement of electronic components, systems, materials, equipment, facilities or related fabrication services. Subscriptions are available through electronics-cooling.com.

INTERESTING TIMES

Ross Wilcoxon
Associate Technical Editor of *Electronics Cooling Magazine*
Senior Technical Fellow, Collins Aerospace MIssion Systems

The ancient Chinese blessing/curse "May you live in interesting times" is neither ancient nor Chinese. I guess whether you consider it a blessing or a curse depends on your perspective and situation. We seem to be in the midst of interesting times, so I thought I would use this editorial to write a few of my thoughts on that.

On one hand, I generally refuse to let myself believe that I'm living through especially challenging or changing times. Any time I begin thinking that way, I envision the eye roll that I would get from my grandparents. By the time they were a few years older than I am today, they had seen two world wars, a great depression, and human flight transition from the Wright brothers to Neil Armstrong. In comparison to those events, my world has seemed to be pretty stable.

On the other hand, factors such as climate change, the ongoing repercussions of the pandemic, and the inability of many politicians around the world to consider anything other than politics, makes it seem that these are particularly 'interesting times'. Adding to the interest level, numerous disruptive technologies are developing and evolving at an uncomfortably fast pace.

Electronics cooling is one discipline being disrupted by many of these technologies and other changes. Data center design, which often drives advances in cooling technologies, is increasingly influenced by the need to reduce the consumption of resources like electricity and water. The transition of some transportation sectors from petroleum-based energy to electrical power requires improved cooling of power electronics and batteries. Mobile electronics are increasingly capable while operating under extremely challenging cooling conditions. Advances in artificial intelligence and machine learning (AI/ML) require new levels of processing power. While the growth of AI/ML may increase processor cooling thermal challenges, they also offer new tools for optimized heat sink geometries and active thermal control.

Throughout its history, the electronics industry has experienced technology disruptions that impact cooling methods. One of these may have slightly affected me – although I did not realize it at the time. About three decades ago, I was a graduate student at the University of Minnesota and my advisor informally loaned me to another professor in the department, Avi Bar-Cohen. I was asked to help one of Prof. Bar-Cohen's students set up a test rig for a two-phase electronics cooling project funded by IBM. After working on this for a couple of months, the project was canceled and I went back to working on my own research. I don't know exactly what factors led the project to be canceled, but that did occur right around the time that the industry saw a 10x reduction in component heat flux due to the transition from bipolar to CMOS logic. While that change may or may not have impacted me, I'm certain that many electronics cooling engineers did experience a significant impact from this substantial, albeit temporary, drop in processor heat flux resulting from new technology.

So interesting times have always been, and always will be, with us. One way to help keep these interesting times more of a blessing than a curse is to keep yourself educated so as to have a better idea of what is coming and what to do about it. I hope that *Electronics Cooling Magazine* helps its readers in that way. This issue's educational opportunities include methods to assess different data center cooling approaches, methods for accurately modeling fans, a comparison of different heat pipe spreader approaches, a method for quickly assessing the thermal capacity of mobile electronics, and a discussion on data analysis approaches.

As always, we editors welcome your feedback and invite you to submit your own article to be included in a future issue.

Ross

cādence®

Celsius EC Solver

Electronics cooling software for optimizing the thermal efficiency of complete systems

LEARN MORE

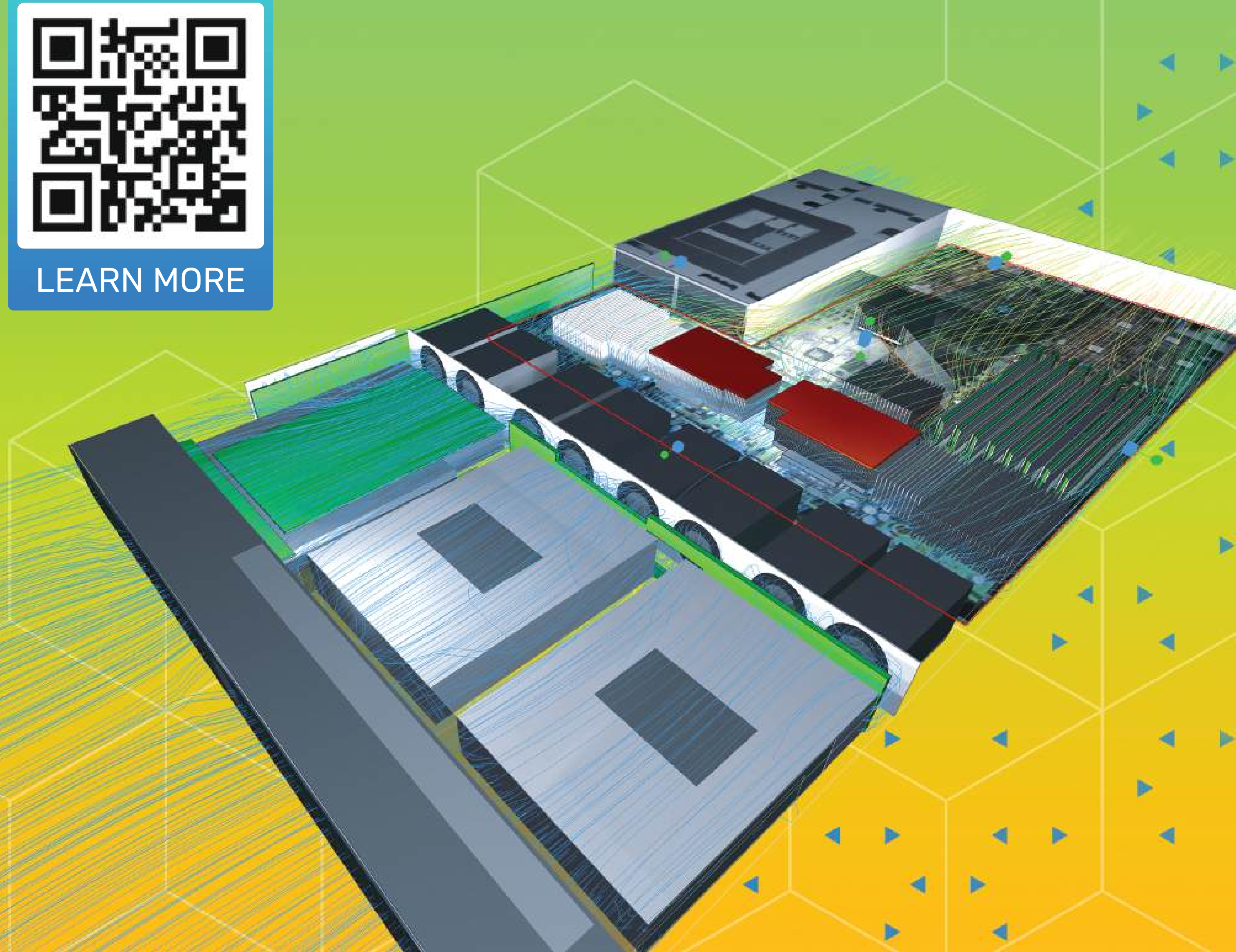

TECHNICAL EDITORS SPOTLIGHT

Meet the 2023 Editorial Board

VICTOR CHIRIAC, PhD | GLOBAL COOLING TECHNOLOGY GROUP

Associate Technical Editor

A fellow of the American Society of Mechanical Engineers (ASME) since 2014, Dr. Victor Adrian Chiriac is a co-founder and a managing partner with the Global Cooling Technology Group since 2019. He previously held technology/engineering leadership roles with Motorola (1999-2010), Qualcomm (2010 – 2018) and Huawei R&D USA (2018 – 2019). Dr. Chiriac was elected Chair of the ASME K-16 Electronics Cooling Committee and was elected the Arizona and New Mexico IMAPS Chapter President. He is a leading member of the organizing committees of ASME/InterPack, ASME/ IMECE and IEEE/CPMT Itherm Conferences. He holds 21 U.S. issued patents, 2 US Trade Secrets and 1 Defensive Publication (with Motorola), and has published over 110 papers in scientific journals and at conferences.

► vchiriac@gctg-llc.com

GENEVIEVE MARTIN | SIGNIFY

Associate Technical Editor

Genevieve Martin (F) is the R&D manager for thermal & mechanics competence at Signify (former Philips Lighting), The Netherlands. She has worked in the field of cooling of electronics and thermal management for over twenty years in different application fields. From 2016 to 2019, she coordinated the European project Delphi4LED, which dealt with multi-domain compact modeling of LEDs and, since 2021, is coordinating the AI-TWILIGHT project. She served as general chair of the SEMI-THERM conference and is an active reviewer and technical committee member in key conferences including SEMI-THERM, Therminic, and Eurosime. She has over 20 journal and conference papers and 16 worldwide patents.

► genevieve.martin@signify.com

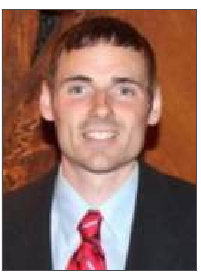

ALEX OCKFEN, P.E. | META

Associate Technical Editor

Alex Ockfen is a simulation engineer at Meta (formerly Facebook), providing technical leadership for thermal and structural design of consumer electronics products. He held previous positions at Raytheon where he obtained experience in thermal management and electronics cooling of a wide range of aerospace and defense applications. He has more than 10 journal and conference publications, is an inventor on multiple patents, is a professional mechanical engineer, and is currently serving as program chair of the SEMI-THERM conference.

► alex.ockfen@fb.com

ROSS WILCOXON | COLLINS AEROSPACE

Associate Technical Editor

Dr. Ross Wilcoxon is a Senior Technical Fellow in the Collins Aerospace Advanced Technology group. He conducts research and supports product development in the areas of component reliability, electronics packaging, and thermal management for communication, processing, displays, and radars. He has more than 40 journal and conference publications and is an inventor on more than 30 US Patents. Prior to joining Rockwell Collins (now Collins Aerospace) in 1998, he was an assistant professor at South Dakota State University.

► ross.wilcoxon@collins.com

COOLING EVENTS

News of Upcoming 2023 Thermal Management Events

ICATMSC 2023
San Francisco, United States

International Conference on Automotive Thermal Management Systems and Control aims to bring together leading academic scientists, researchers and research scholars to exchange and share their experiences and research results on all aspects of Automotive Thermal Management Systems and Control. It also provides a premier interdisciplinary platform for researchers, practitioners and educators to present and discuss the most recent innovations, trends, and concerns as well as practical challenges encountered and solutions adopted in the fields of Automotive Thermal Management Systems and Control.

Desc. source: electronics-cooling.com
►**https://waset.org/automotive-thermal-management-systems-and-control-conference-in-september-2023-in-san-francisco**

THERMINIC 2023
Budapest, Hungary

The 29th THERMINIC Workshop in Budapest, Hungary. THERMINIC is the major European Workshop related to thermal issues in electronic components and systems.
This year’s event again promises to be a very special occasion with a high-quality programme and exciting social events. The technical programme will include oral talks, poster presentations, special sessions and invited keynote talks given by renowned speakers. This time, we will again offer professional development courses (PDCs) on the day before the workshop.

We look forward to welcoming you to Buapest this coming September!

Desc. source: electronics-cooling.com
►**https://therminic2023.eu/**

SAE 2023 Thermal Management Systems Symposium
Plymouth, Michigan

During this time of technical transition and transformation to advanced propulsion, it is more important than ever to have access to timely, relevant information and updates in the areas of cutting-edge technology, standards, regulations, and testing to inform and align strategic initiatives. The ongoing goal is to reduce engine emissions, conserve energy, dissipate heat, reduce noise, improve the cabin environment, and increase the overall vehicle performance. Only the SAE 2023 Thermal Management Systems Symposium (TMSS) provides you critical access directly to the industry's leading experts who are ready to share their latest innovations and solutions.

At TMSS you will engage with engineers from OEMs, Tier 1 & 2 suppliers, regulatory entities, and other discrete part developers from around the globe to discuss industry trends, the latest thermal management and climate control strategies, developments, and systems integration,

and still to-be-developed technology impacting thermal systems management. Here, you will have the opportunity to communicate your concerns, issues, and possible solutions pertaining to current and proposed regulations.

TMSS is where important conversations happen. Don't miss this vital opportunity to interact with and network the best of the best in the field of ground vehicle thermal systems technology and thermal systems management.

Desc. source: electronics-cooling.com
►**https://www.sae.org/attend/thermal**

Thermal Live Fall Summit 2023
Available On Demand at thermal.live

Thermal Live Fall Summit is a two-day, online event that features webinars and product demos from industry experts! Join us for an event that will be a resource for you now, in the future, and implemented into your standard, every day practices.

Desc. source: electronics-cooling.com
►**thermal.live**

Summary of SEMI-THERM 2023 Conference

Marcelo del Valle
General Chair of SEMI-THERM
Infinera Corporation

Lieven Vervecken
CEO and Co-Founder of Diabatix

Alex Ockfen, P.E.
Simulation Engineer at Meta

The SEMI-THERM 39 Symposium was held March 13-16, 2023 at the Double Tree Hotel in San Jose, CA. Program organization was led by General Chair Marcelo del Valle (Infinera Corporation), Program Chair Alex Ockfen (Meta), and Program Vice Chair Lieven Vervecken (Diabatix). The Symposium included technical short courses, technical sessions, invited presentations, vendor exhibits and workshops, a 'how-to' session, a panel discussion, luncheon talks, and an industry tour.

Five short courses were held on Monday, March 13. These courses were selected to provide learning opportunities for individuals ranging from those who are new to thermal design to those who are highly experienced. These courses were offered:

- "Fundamentals of CFD for Heat Transfer Analysis: Governing Equations, Numerical Methods, and Applications", taught by Ine Vandebeek and Lieven Vervecken of Diabatix.
- "Understanding, Applying and Estimating the Performance of Advanced Two-phase Heat Pipe Systems", taught by Olivier de Laet and Vincent Dupont of Calyos SA.
- "Addressing Chip Component Thermal and Reliability Challenges for Qualification of Liquid-Cooled Compute System for Autonomous Driving", taught by Fen Chen of Cruise LLS.
- "Direct to Chip Liquid Cooling: Single Phase Water Versus Pumped Two-Phase Refrigerant Cooling", taught by Prof. Alfonso Ortega of Villanova University.
- "Transient Thermal Analysis Using Linear Superposition", taught by Roger Stout (retired from ON Semiconductor).

Marcelo del Valle

Dr. Marcelo del Valle is a Staff Hardware Development Engineer for the Optical Modules Group at Infinera Corporation. Before joining Infinera, he worked as Staff Thermal Engineer at ZT systems where he designed cooling solutions for rack mounted servers. Additionally he worked as a Thermal Mechanical Engineer at Intel corporation where he developed air and liquid cooling solutions for the Omni-Path HPC network equipment product line. Dr. Del Valle holds a B.S.M.E from Universidad de Santiago, Chile, a M.S.M.E. from University of Nevada, Reno and a Ph.D. in Mechanical Engineering from Villanova University. He has worked extensively in experimental measurements in the thermal sciences for more than 10 years. He has published and presented extensively in problems arising from thermal management of electronics, spanning from the chip/module to the facility level, single and two-phase cooling, and thermal management in energy systems.

Dr. Lieven Vervecken

Dr. Vervecken is the CEO and co-founder of Diabatix, a software company specialized in advanced thermal design. Prior to founding Diabatix, Dr. Vervecken received a Ph.D. in mechanical engineering from the renowned KU Leuven in the field of numerical simulations. Dr. Vervecken incorporated his expertise into the advanced A.I. technology at the heart of Diabatix. What started as a small venture has become a fast-growing SaaS company serving multinationals worldwide. Dr. Vervecken is the lead author of multiple peer-reviewed journal articles and an experienced keynote speaker at national and international conferences.

Alex Ockfen, P.E.

Alex Ockfen is a simulation engineer at Meta (formerly Facebook), providing technical leadership for thermal and structural design of consumer electronics products. He held previous positions at Raytheon where he obtained experience in thermal management and electronics cooling of a wide range of aerospace and defense applications. He has more than 10 journal and conference publications, is an inventor on multiple patents, is a professional mechanical engineer, and is currently serving as program chair of the SEMI-THERM conference.

The technical conference was held Tuesday, March 14 - Thursday, March 16. Fourty-two presentations were included in the nine technical tracks comprised of twelve different sessions:

- Comfort and Compliance
- Two Phase Cooling (two sessions)
- Advanced Manufacturing and Materials
- Emerging Technologies
- Immersion Cooling
- Testing & Measurement Methods (two sessions)
- Thermal Interface Materials (two sessions)
- Data Centers
- Numerical Modeling Methods
- Immersion Cooling

The technical program also included three invited presentations by recognized industry leaders:

- Ashish Guptao, of Intel, made the Keynote presentation on "Sustainable Solutions: Liquid Cooling in Data Centers", which discussed the environmental benefits and latest innovations of implementing more liquid cooling into data centers.
- Veerendra Mulay, of Meta, was recognized for winning the SEMI-THERM 39 Thermi Award. His presentation "This journal is 1% finished" gave his perspective on his engineering journey (so far).
- Alfonso Ortega, of Villanova University, was recognized for winning the SEMI-THERM 39 Hall of Fame Award. His presentation "Thermal Management of Electronic Systems 1970-2023: An Academic Perspective" discussed the evolution of electronics cooling as it transitioned from liquid cooling to air cooling and now back to liquid cooling with two-phase flow.

The Best Paper Award was given to "Performance Comparison of Five Data Center Server Thermal Management Technologies" by Tim Shedd and Emily Clark of Dell Technologies. An adaptation of this paper is featured in the Summer 2023 Issue of *Electronics Cooling Magazine.*

Other technical papers recognized included:

- "Experimental Performance of Supercritical Carbon Dioxide within Cold Plates made with Additive Manufacturing Techniques" by Wyatt Stottlemyre, Alec Nordlund, Joshua Gess (Oregon State University), Bharath Ramakrishnan, Ruslan Nagimov, Husam Alissa (Microsoft) - 2nd place.
- "Thermal Conductivity is NOT the Only Deciding Factor: A Guide to Understanding Unaddressed Challenges with Liquid Metals TIMs", by Claire K. Wemp and John N. Hodul (DuPont Silicon Valley Technology Center) - Honorable mention.
- "Reduced-Order Modeling for Thermal Dose Forecasting in Wearable Devices", by Harry A. J. Watson, May Yen and Francesco Colella (Exponent, Inc.) - Honorable mention.
- "Fractional Thermal Runaway Calorimetry", by May Yen, Artyom Kossolapov, Sergio Mendoza, and Francesco Colella (Exponent, Inc.) - Honorable mention

A critical aspect of the SEMI-THERM Symposium is the strong role that vendors play. Thirty nine companies participated in the two-day Vendor Exhibits, which included industry leaders in thermal devices such as heat sinks, thermal interface materials, heat pipes and vapor chambers, fluid connectors, air-movers, systems, and advanced materials. Other exhibitors featured tools for thermal simulation and testing, thermal consulting, a university consortium and, of course, *Electronics Cooling Magazine*. In addition to the booths in the exhibit hall, a number of vendors also gave Vendor Workshops in which they provided detailed information on their products in a more formal presentation format.

Other SEMI-THERM 39 activities included:

- The DuPont Silicon Valley Technology Center (SVTC) hosted a facility tour for SEMI-THERM attendees. This tour included visiting 10 applied engineering labs and the innovation center to meet with SVTC engineers to discuss thermal management and RF technologies.
- Herman Chu (Celestica) gave a 'How-To' presentation entitled "A Look at Acoustic Fundamentals and Designs as Applied to Air-Cooled Electronics" that provided an overview of important factors to consider in addressing the acoustic effects of cooling fans.
- In the panel discussion "Career Trajectories in Thermal Design" invited speakers provided their thoughts and recommendations to individuals who are early in their careers in the industry. The panel was moderated by Taravat Khadivi (Meta) and included Ross Wilcoxon (Collins Aerospace), Yueming Li (Meta), Lieven Vervecken (Diabatix) and Nicole Okamoto (San Jose State University) as panelists.

- Invited speakers gave informational and entertaining luncheon presentations on the first two days of the Symposium. On Tuesday March 14, Katrien Herdewyn, founder of Elegnano, described how her company applies nanotechnology to shoes in her presentation entitled “High Tech in High Heels”. On Wednesday March 15, Jousef Murad, founder of APEX, described how he uses social media in his role as an engineering influencer.
- The Harvey Rosten Award, which is sponsored by Siemens Digital Industries Software, is presented at SEMI-THERM. This year’s winner was “Analysis of the Thermal Behavior of Li-Ion Pouch Battery Cell – Part II: Circuit-based Modeling for Fast and Accurate Thermo-Electrochemical Simulation”, by Antonio Pio Catalano. Ciro Scognamillo, Francesco Piccirillo, Pierluigi Guerriero, Vincenzo d’Alessandro and Lorenzo Codecasa. The paper was presented at the 2022 28th International Workshop on Thermal Investigations of ICs and Systems (THERMINIC).

About SEMI-THERM

The first SEMI-THERM was first held Phoenix, AZ in 1984 with a goal of fostering networking opportunities for industry and academic professionals in semiconductor thermal management. Ultimately, the SEMI-THERM Educational Foundation (STEF) was established in 2013 as a Non-Profit Educational Foundation. STEF is dedicated to worldwide educational opportunities and resources within the electronics thermal engineering community, with a goal of providing programs for on-going professional development, technical networking, and engagement of academia and industry in pursuit of innovation and excellence.

More information on SEMI-THERM is available on **https://semi-therm.org/.**

SEMI-THERM 40 will be held in San Jose, CA, March 25-29, 2024.

Calculating Thermal Design Power for Mobile Consumer Electronics – Part 2

Alex Ockfen, P.E.
Simulation Engineer at Meta

Overview

Thermal Design Power (TDP) is a term commonly used in the thermal management of consumer electronics. While the usage of this terminology may vary across the industry, it commonly refers to the amount of power that a device may dissipate indefinitely, in a given thermal environment, without exceeding the temperature limits of the device. The TDP for a consumer electronics device is of great interest because it provides physical bounds to the experience a product can deliver to the user (e.g., phone call, internet, photo capture, gaming, etc.).

Thermal design engineers often have the most influence on a product's design during its architecture development. It is not uncommon for designs to rapidly evolve in this phase of the design cycle, with real-time changes occurring daily or even hourly. It is also not uncommon for teams to rapidly pivot between multiple concepts. Some first-order tools are essential to provide effective thermal design guidance in a fast-paced environment. Detailed finite element or computational fluid dynamics simulations are often not practical due to the timeline and lack of design maturity. TDP provides one simple and useful metric that can guide the design in the desired direction.

Where We Left Off

A physics-based method for determining the thermal design power of a passively cooled consumer electronics tablet with in-plane thermal gradients was provided in Part 1 of this column [3]. The thermal design power of a device like that shown in *Figure 1* can be calculated using *Equation 1*, where h is the effective heat transfer coefficient, A is the external area of the device, T_{limit} is the touch temperature limit, $T_{ambient}$ is the ambient operating temperature, and the CTS is the coefficient of thermal spreading [1].

$$TDP = hA(T_{limit} - T_{ambient})CTS \qquad \{1\}$$

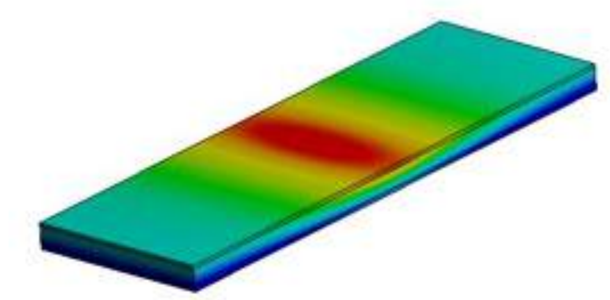

Figure 1 - Isotherm on an example tablet or mobile phone product

When in-plane thermal gradients dominate and the temperature on the front and back surfaces of the device are identical, the CTS can be quantified using the fin equation.

Through-Plane Thermal Gradients

Additional thermal design tools are needed to account for through-plane thermal gradients that develop across the thickness of the device. Even when there are minimal in-plane thermal gradients, a CTS correction to the theoretical thermal design power is required when the front and back surfaces of the device are at different temperatures.

Alex Ockfen, P.E.
Meta
Alex Ockfen is a simulation engineer at Meta (formerly Facebook), providing technical leadership for thermal and structural design of consumer electronics products. He held previous positions at Raytheon where he obtained experience in thermal management and electronics cooling of a wide range of aerospace and defense applications. He has more than 10 journal and conference publications, is an inventor on multiple patents, is a professional mechanical engineer, and is currently serving as program chair of the SEMI-THERM conference.

The thermal design power is determined when any point on the surface of the device reaches the temperature limit. Thus, if one side of the device reaches the temperature limit before the other, the device's ability to reject heat to the environment is reduced. *Figure 2* provides a cross-section of a device with different temperatures on its front and back surfaces.

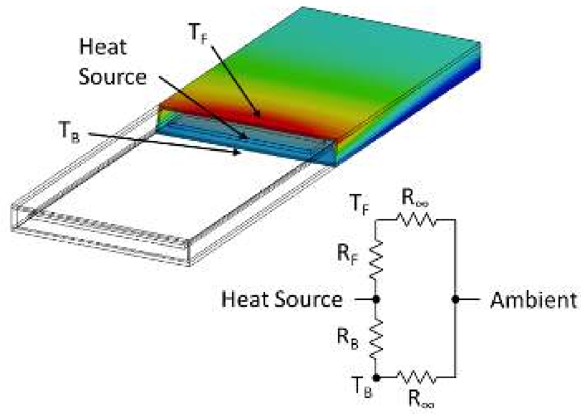

Figure 2 - Isotherm showing thermal imbalance between front and back of a notional product

Approach for Calculating CTS with Through-Plane Thermal Gradients

The primary heat source in many consumer electronics products is an electronic component, such as a processor, that is centrally located in the product and mounted on a printed circuit board assembly (PCBA). The thermal architecture of the product defines the heat paths between this heat source and the front and back surfaces of the product, which reject heat to the environment.

One method to evaluate the coefficient of thermal spreading with through-plane thermal gradients is to calculate the thermal resistance values from the heat source to the front (R_F) and back (R_B) surfaces of the device respectively. The reader is referred to a heat transfer text, such as *Reference [2]*, for details on calculating equivalent resistances through composite structures. For example, the resistance from the heat source to the front of the device may include transfer through a thermal interface material, into a chassis, and then to the surface of the device.

Once the resistances to the front and back surfaces of the product are calculated, the parallel thermal resistance network illustrated in *Figure 2* can be used to determine the temperature difference across the thickness of the device, as well as the heat rejected to each surface. The multiplier ($M_{through\text{-}plane}$), defined in *Equation 2*, falls out of the parallel resistor network, where R_F is the resistance to the front surface of the product, R_B is the resistance to the back surface of the product, and R_∞ is the thermal resistance between the device surfaces and the external environment.

$$M_{through-plane} = \frac{1}{1+\frac{ABS(R_B-R_F)}{(R_B+R_F+2R_\infty)}} \qquad \{2\}$$

This multiplier quantifies the reduction in thermal design power attributed to through-plane thermal gradients. *Figure 3* illustrates this multiplier as a function of the non-dimensional resistance ratio R_{eq}/R_{max}. R_{eq} is defined by *Equation 3* and represents the total equivalent thermal resistance from the heat source to the environment (including both front and back surfaces). R_{max} is defined by *Equation 4* and represents the larger of the thermal resistances between the heat source and the environment (through either the front <u>or</u> back surfaces individually).

$$R_{eq} = \frac{(R_B+R_\infty)(R_F+R_\infty)}{(R_B+R_F+2R_\infty)} \qquad \{3\}$$

$$R_{max} = MAX[(R_B + R_\infty), (R_F + R_\infty)] \qquad \{4\}$$

When the front and back thermal resistances are equal ($R_{eq}/R_{max} = 0.5$), the multiplier equals 1 and the theoretical maximum thermal design power is achieved. When the thermal resistance to one surface of the device is much greater than to the other, the multiplier approaches 0.5, and essentially only one surface of the device is used for heat rejection. The magnitude of multiplier variation illustrates the importance of through-plane thermal gradients in the product design process.

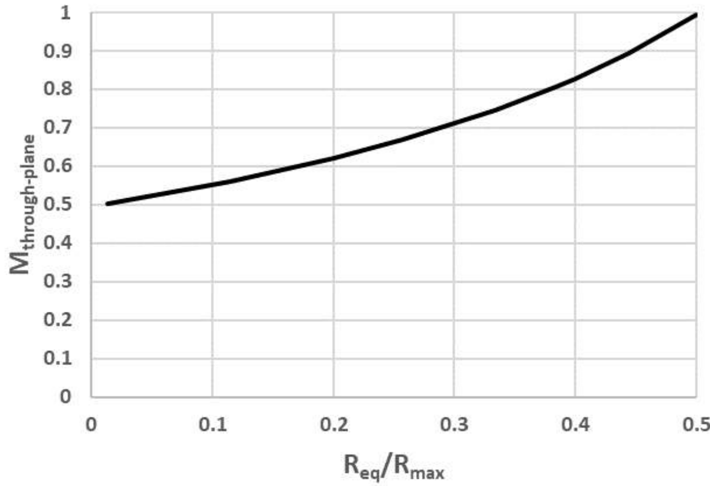

Figure 3 - Through-plane multiplier as a function of front-to-back resistance imbalance

When a product with negligible in-plane thermal gradients exhibits a temperature difference between its front and back surfaces, the CTS becomes equivalent to the through-plane multiplier in *Equation 5*.

$$CTS = M_{through-plane} = \frac{1}{1+\frac{ABS(R_B-R_F)}{(R_B+R_F+2R_\infty)}} \qquad \{5\}$$

Putting it into Practice

Now let's demonstrate this for the calculation on a notional device with the inputs specified in *Table 1* and negligible in-plane thermal gradients. It is common for the environment, temperature limits, and form factor to be known early in the design process.

INPUT	VALUE	UNITS
T_{limit}	45	°C
$T_{ambient}$	25	°C
h	10	W/m^2C
A*	7500	mm^2
* Area is for 1 side (front or back surface)		

Table 1 - Inputs for calculation

A cross-section of the notional device is provided in *Figure 4*. Heat is assumed to be generated on a PCB in the middle of the device. Heat leaving the front surface of the device passes through a thermal interface material (TIM) and a chassis. Heat leaving the back of the device passes through an air gap and the device battery. The thickness (t) and thermal conductivity (k) of each layer is specified in *Figure 4*, with all layers assumed to remain constant in the plane of the device.

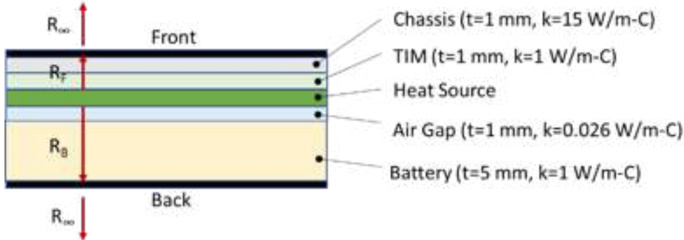

Figure 4 - Cross-section illustrating heat paths in a notional device

The thermal resistance in each individual layer is calculated using the one-dimensional resistance equation for heat conduction through a medium, t/kA. The resistance to the front and back of the device is calculated by combining the individual layer resistance values; this is achieved via a simple sum when the individual resistors are in series. As an example, the thermal resistance to the front of the device is the sum of the chassis and thermal interface material layers.

The resistance to the environment is calculated using the thermal resistance equation, 1/hA. Note that the effective heat transfer coefficient (h) in this equation must account for all heat rejection modes. In this example, the value is based on the sum of an empirical correlation for natural convection and a linearized radiation heat transfer coefficient.

The total equivalent resistance from the heat source to the environment (R_{eq}) of 7.91 °C/W is calculated via *Equation 3* and the maximum thermal resistance of 19.13 °C/W is calculated via *Equation 4*. The maximum thermal resistance occurs through the heat path out of the bottom of the device and is driven by the air gap between the heat source and the battery.

PARAMETER	EQUATION	VALUE	UNIT
$R_{chassis}$	t/kA	0.01	°C/W
R_{TIM}	t/kA	0.13	°C/W
$R_{battery}$	t/kA	0.67	°C/W
R_{air}	t/kA	5.13	°C/W
R_F	$R_{chassis} + R_{TIM}$	0.14	°C/W
R_B	$R_{battery} + R_{air}$	5.79	°C/W
R_∞	1/hA	13.33	°C/W
R_{eq}	Equation 3	7.91	°C/W
R_{max}	Equation 4	19.13	°C/W

Table 2 - Resistance calculation

The resulting through-plane multiplier of 0.85 is calculated using *Equation 2*. Alternatively, the multiplier can be read directly from *Figure 3* using the calculated resistance ratio of 0.41 (R_{eq}/R_{max}). The resulting TDP for the device, when corrected for through-plane thermal gradients, is 2.55 Watts *(Table 3)*. This is lower than the ideal TDP of 3.00 Watts. If additional thermal capability is required, the thermal designer can iterate this process to converge on a more satisfactory set of design parameters (e.g., balance heat paths via through-thickness gaps, materials, etc.).

PARAMETER	EQUATION	VALUE	UNIT
R_{eq}/R_{max}	R_{eq}/R_{max}	0.41	-
$M_{thru\text{-}plane}$	Equation 2	0.85	-
TDP_{ideal}	Equation 1*	3.00	W
$TDP_{corrected}$	Equation 1	2.55	W
* Isothermal assumption, CTS = 1			

Table 3 - TDP calculation

Concluding Remarks

This first-order method provides the thermal engineer with a tool to quickly estimate the thermal design power limit for devices that experience though-plane thermal gradients. This approach is well suited for architecture studies in which the design rapidly evolves and estimates are needed to guide the design team. While this method can be very useful, it does not replace detailed design and validation. It is instead intended to refine design concepts before transitioning to more detailed simulations and/or tests.

Since real products experience through-plane and in-plane thermal gradients simultaneously, future work is planned to combine the tools provided in Parts 1 and 2 of this column to enable readers to account for both through-plane and in-plane thermal gradients simultaneously in their thermal design power calculations.

References

[1] Victor Chiriac, "A Figure of Merit for Smart Phone Thermal Management", Electronics Cooling Magazine, April 2017

[2] Frank Incropera and David DeWitt, Fundamentals of Heat and Mass Transfer, 4th Edition, Wiley (1996)

[3] Alex Ockfen, "Calculating Thermal Design Power for Mobile Consumer Electronics – Part 1", Electronics Cooling Magazine, February 2023

Advanced Cooling System for Modular Electronics Thermal Management

Sai Kiran Hota
R&D engineer II at ACT

Greg Hoeschele, Srujan Rokkam, Kuan-Lin Lee
Principal Materials Engineers at ACT

Introduction

Modern electronics are rapidly evolving to meet high-computing needs while shrinking in size resulting in large heat fluxes that must be removed for safe operation. *Figure 1* shows a schematic of a generic electronics cooling system with representative heat transfer pathway from a chip (heat source) to a cold plate (heat sink) via heat spreaders and card retainers (e.g., Wedge-loks).

Heat spreaders are the first thermal link that remove heat from the electronic chips directly and transfer it to a chassis via mechanical card retainers, which expand in one-direction, that are commonly called wedge-loks. The heat is further dissipated from the chassis to an enclosure heat sink (shown in *Figure 1* is a cold plate-based heat sink). Conventional cooling systems with aluminum plate-spreaders with limited thermal conductivity (k≈180 W/m-K) and conventional wedge-loks are incapable of maintaining electronics temperature below 70°C at high heat fluxes. To address this challenge, it is necessary to explore alternative cooling solutions for the next generation of high-performance computing systems. Two-phase heat spreaders, such as *Embedded Heat Pipe* (EHP) and *Pulsating Heat Pipe* (PHP) plates, along with thermally enhanced wedge-loks that expand diagonally (i.e., two directions) are alternative high-performance options. This article will first discuss each of these components and provide general (design) guidelines.

Sai Kiran Hota
Sai Kiran Hota is an R&D engineer II at ACT. He received his Ph.D. in Mechanical Engineering in 2021 and then joined ACT. Dr. Hota has worked primarily on developing thermal management technologies funded by various government agencies including Department of Energy and NASA. He is actively working on developing pulsating heat pipes for space and terrestrial applications at ACT.

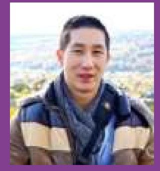

Kuan-Lin Lee
Dr. Kuan-Lin Lee is a highly accomplished engineer with expertise in two-phase thermal management technologies. He joined ACT in 2016 after receiving his Ph.D. in Case Western Reserve University. He is currently leading an R&D team at ACT to develop advanced cooling technologies for future space and terrestrial applications, such as 3D printed pulsating heat pipes for space electronics, advanced heat pipes for lunar landers and rovers, alkali metal heat pipe for Hall thruster and advanced two-phase PCM heat sink for Smallsats.

Greg Hoeschele
Mr. Greg Hoeschele is the Lead Engineer in the Passive Heat Exchangers Product Development Group. Prior to joining ACT, Mr. Hoeschele worked as a design engineer in the innovative fuel cell industry. Once at ACT, Mr. Hoeschele used his skills to lead multiple thermal programs within the diverse Industrial Products market. Upon transitioning to the lead role, Mr. Hoeschele has taken on all heat pipe, phase change material, and liquid cold plate development projects. Mr. Hoeschele received his B.S. in Mechanical Engineering from Lafayette University and his Masters in Mechanical Engineering from Cornell.

Srujan Rokkam
Dr. Srujan Rokkam is an Engineering Manager of Research and Development Group at ACT. He joined ACT in 2012, after receiving Ph.D. in Mechanical Engineering. His research work in the last 16 years has been at the intersection of materials modeling, thermal management, energy systems and computational science. At ACT, he leads a group of 20+ people focused on development of new thermal fluid technologies for applications in areas of spacecraft thermal management, two-phase heat transfer, avionics cooling and energy systems. Dr. Rokkam has led over 20 SBIR/STTR projects and successfully transitioned two projects through post-Phase II technology transition.

Subsequently, a study comparing an advanced electronics cooling system with two-phase heat spreaders and enhanced wedge-loks against the current state-of-the-art system is presented.

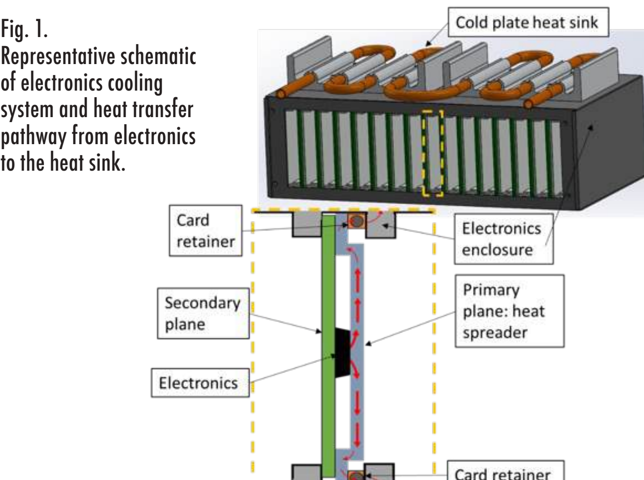

Fig. 1. Representative schematic of electronics cooling system and heat transfer pathway from electronics to the heat sink.

Nomenclature

$\beta_{vapor-inertial}$	PHP working fluid transport factor
ρ_l	Liquid density
ϵ	Surface roughness/ nucleation cavity size
σ	Surface tension
h_{fg}	Enthalpy of vaporization
μ_l	Viscosity of liquid
C_{pl}	Specific heat capacity of liquid
$\partial P/\partial T$	Saturation pressure gradient against temperature
Z	Compressibility factor
R	Gas constant
T_{sat}	Saturation temperature

Advanced Passive Electronics Heat Spreader Technologies

Embedded Heat Pipe (EHP) Heat Spreader

An EHP heat spreader is comprised of heat pipes embedded in an aluminum baseplate, to result in a high conductivity plate [1]. *Figure 2 (a)* shows the schematic of operation of the heat pipe. A heat pipe is a device that utilizes evaporation and condensation of a working fluid inside a sealed container for heat delivery: Heat applied on one end (evaporator side) is transported to the other end by the vapor resulting from phase transition of the working fluid. The vapor condenses at the other end (i.e., condenser side) and the condensation returns to the evaporator by capillary forces. Further details on the heat pipe operation can be accessed in [2]. Typically for an EHP plate, heat pipes made of copper tube are used with a compatible working fluid. The working fluid is selected based on the Figure of Merit (FOM), which is a fluid property derivative from the capillary limit [3]:

$$FOM = \frac{\rho_l \sigma h_{fg}}{\mu_l} \qquad [3]$$

Figure 2 (b) shows the FOM of various fluids for heat pipes. Generally, electronics operate in the range of -20°C to 70°C. In this operating temperature range, water is the best heat pipe working fluid, followed by ammonia. Water is also compatible with copper, so Cu-H_2O heat pipe is a common choice for EHP in electronics cooling applications. A tool that can help a designer to determine appropriate heat pipe size and wick structure is available in [4].

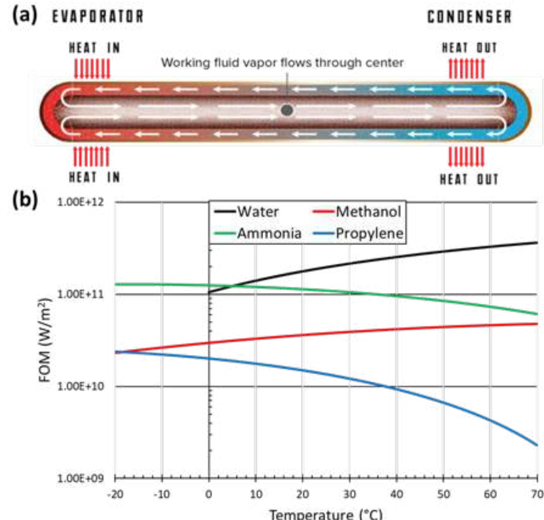

Fig. 2. - Schematic of operation of heat pipe in an EHP, (b) Figure of merit for fluid selection in a heat pipe

Pulsating Heat Pipe (PHP) Heat Spreader

Compared to a heat pipe, a PHP is an emerging passive heat transfer device. Instead of using a wick to return liquid, a PHP uses pulsations (or oscillations) of the working fluid inside a meandering capillary-sized channel connected end to end, as shown in *Figure 3 (a)*, to transport thermal energy. A distinct requirement of the PHP is that the serpentine channel diameter must be smaller than the critical diameter, dictated by the Bond number limit (<4), so that the working fluid inside the channel naturally distributes into liquid slugs and vapor plugs. Heat applied to one end is transported to the other end utilizing fluid pulsations/ oscillations of liquid slug-vapor plug pairs. Further details on the operation of PHP can be accessed in [5].

The selection of a PHP working fluid should consider multiple factors, including Figure of Merit (FOM), fluid transport factor ($\beta_{vapor-inertial}$) and minimum superheat for start-up ($\Delta T_{super-heat}$). The FOM for PHP working fluid selection is based on the thermal performance of a PHP based on fluid properties, as discussed in work of Kim et. al. [6]:

$$FOM = \frac{\rho_l C_{pl} \left(\frac{\partial P}{\partial T}\right)_{sat} ZRT_{sat}}{h_{fg}\mu_l} \qquad [6]$$

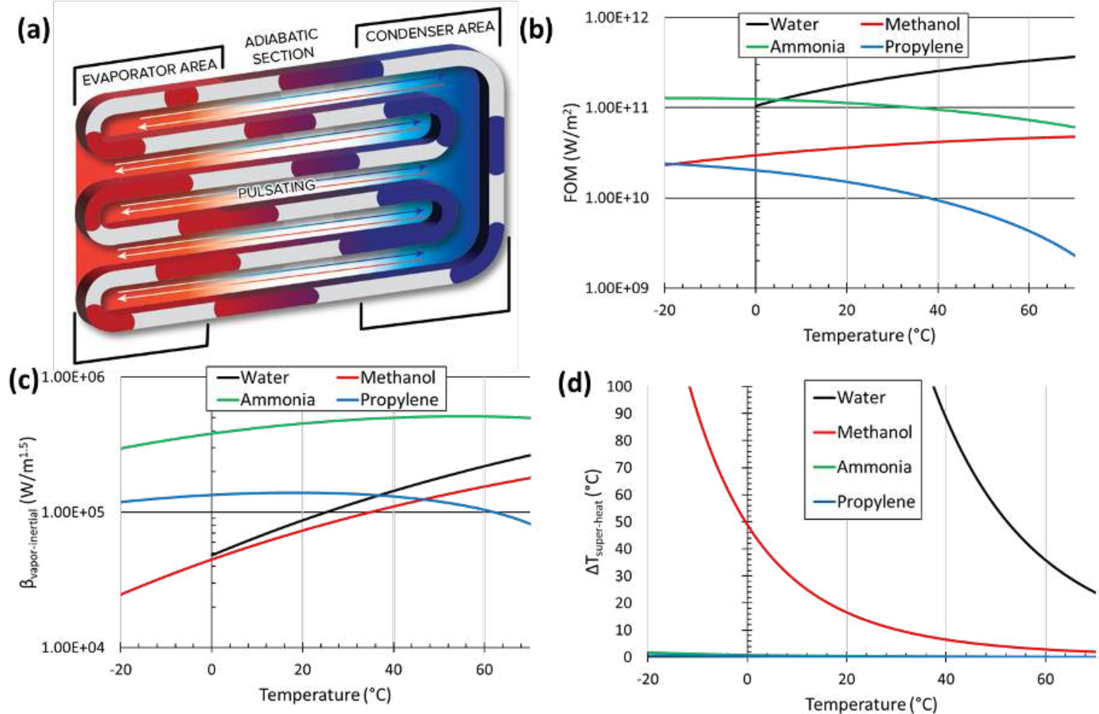

Fig 3. (a) - Schematic of operation of PHP; (b) FOM for PHP based on heat transfer performance; (c) Fluid transport factor limit for PHP; (d) Start-up limit of PHP (assuming channel surface roughness ~ 4μm)

Figure 3 (b) shows the performance-based FOM for various PHP working fluids. Ammonia appears to be the best working fluid, closely followed by propylene. Water and alcohols are less suitable as they require high superheat compared to refrigerants. In addition to high heat transfer performance, the selected working fluid should also enable a PHP to handle higher heat fluxes and have an easier start-up. The maximum heat transfer capability, also called the transport factor ($\beta_{vapor\text{-}inertial}$), can be estimated by the following equation presented in [7]:

$$\beta_{vapor-inertial} = h_{fg}(\sigma\rho_v)^{0.5} \qquad [7]$$

The minimum superheat required for PHP start-up based on nucleate boiling is estimated using [8]:

$$\Delta T_{super-heat} = \frac{2\sigma}{\epsilon}\frac{T}{h_{fg}\rho_v}\left(\frac{\rho_l}{\rho_l-\rho_v}\right) \qquad [8]$$

In summary, it is desirable to select a working fluid for PHPs with a higher FOM and transport factor while requiring a lower superheat to startup. *Figure 3 (c)* shows $\beta_{vapor\text{-}inertial}$ for PHP working fluids, where it is evident that ammonia is the best working fluid within the operating temperature range of -20°C to 70°C. This is followed by propylene, which has a decreasing trend after 40°C.

Figure 3 (d) shows the superheat requirement for the start-up of the PHP. The curves show water and alcohols have significant superheat requirements while refrigerants are more favorable for faster start-up. From a thermal performance perspective, ammonia should be considered as the most suitable working fluid within this operating temperature range. Propylene is the second-best option. Other factors such as safety, structural, compatibility also need to be considered, depending on different operational scenarios. For example, the PHP prototypes developed, tested and discussed in the remaining sections were charged propylene due to safety considerations.

Thermal Performance Comparison of EHP and PHP Heat Spreaders

Figure 4 (a) shows the heat spreaders tested, which had two center heaters (red section) with edge condensers (blue section). A quasi-steady state testing method was adopted with incremental heater power. The size of the heat spreaders was 233 mm x 160 mm x 3.55 mm. Further details on the heat spreaders can be found in [9]. The thermal conductance was calculated as [9]:

$$C = \frac{Q}{\Delta T} \qquad [9]$$

Where, Q is heater power, and ΔT is average temperature difference between evaporator and condenser temperatur

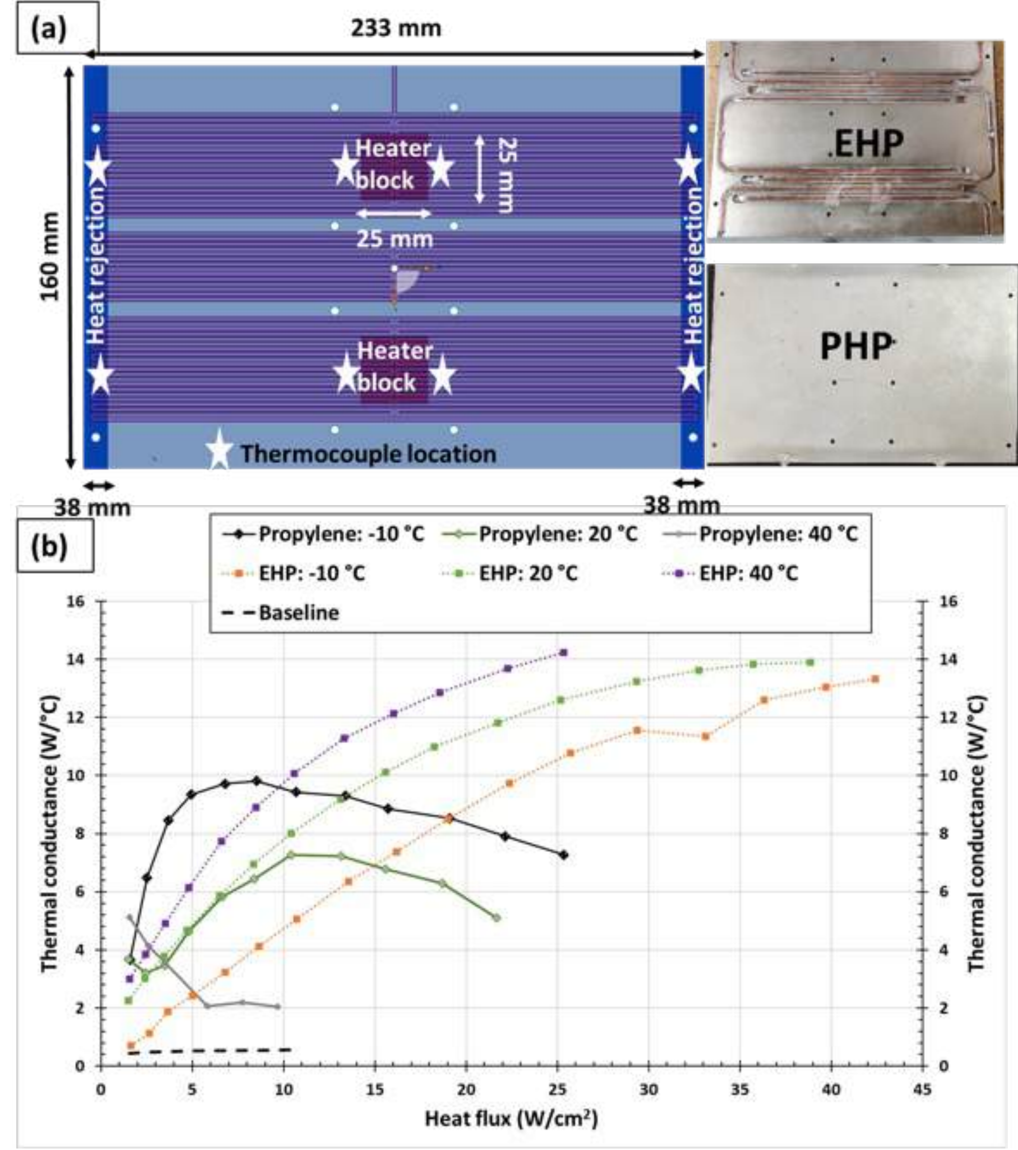

Fig. 4. (a) - Schematic of the test setup for Heat Spreaders Performance Comparison. The prototype EHP and PHP heat spreaders are shown. The dimensions of the heat spreader were 230 mm x 160 mm x 3.55 mm. This corresponds to a 6U-standard electronics card form factor; (b) Thermal conductance comparison plots of the EHP and PHP heat spreaders.

Figure 4 (b) shows the thermal conductance (C) of the heat spreaders at different coolant circulation temperatures. The black dashed line represents the baseline (empty PHP) thermal conductance of 0.5 W/°C. The thermal conductance of the PHP is represented by solid lines with markers and the thermal conductance of the EHP is represented by dotted lines with markers. At low temperature, the PHP with propylene showed higher thermal conductance compared to the EHP, up to a heat flux of 19 W/cm^2. The maximum PHP thermal conductance recorded was > 9 W/°C (18 times more than the baseline). At higher heat flux, the PHP operated in partial dry-out mode with decreasing thermal conductance, while that of the EHP increased up to 13.3 W/°C with a heat flux of 42.4 W/cm^2. The propylene PHP had better or similar performance compared to EHP at lower heat fluxes and at lower set point temperature. Otherwise, the EHP showed superior thermal performance as a heat spreader.

Enhanced Card Retainer (ICE-Lok) for Improved Junction Thermal Conductance

The heat spreader is connected to the electronics chassis by a card retainer (i.e., wedge-lok). As the torque applied to the retainer increases, the wedges expand and make contact with chassis slots to provide a heat transfer pathway between the surfaces. *Figure 5 (a.1)*

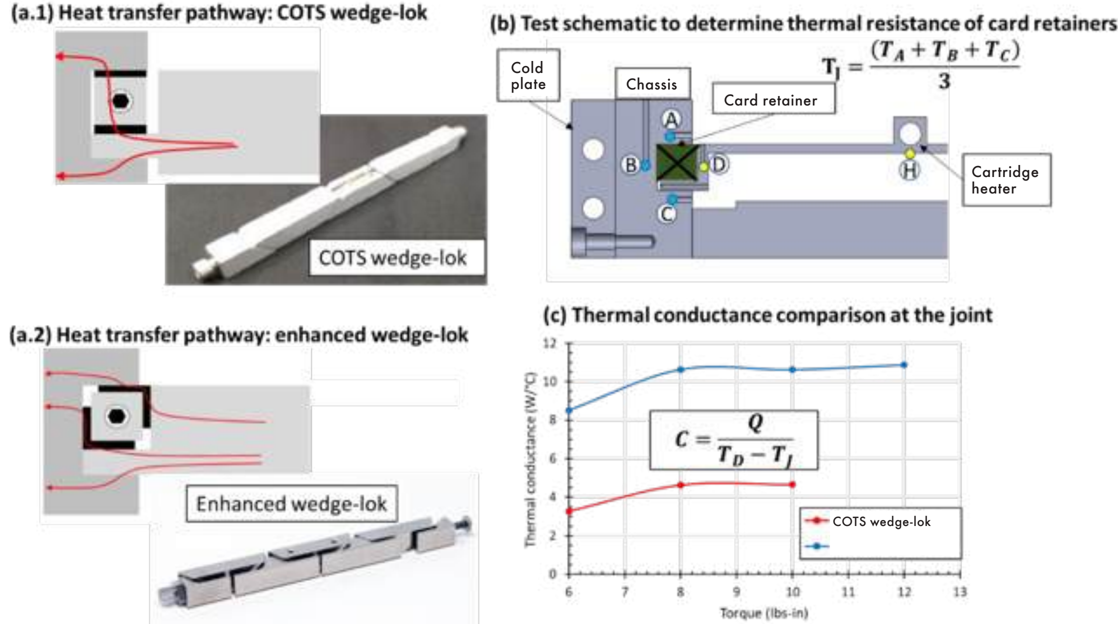

Fig. 5. (a.1) - Heat transfer pathway of a COTS Wedge-Lok [11], image of COTS Wedge taken from [12]; (a.2) Heat transfer pathway of improved card retainer (enhanced wedge-lok) [11]; (b) Test schematic to determine thermal resistance of card retainers; (c) Thermal conductance comparison of the card retainers at the joint

shows the heat transfer pathway in a commercial-Off-The-Shelf (COTS) wedge-lok. An improvement over a COTS wedge-lok is an enhanced wedge-lok, or ICE-Lok, shown in *Figure 5 (a.2)* [10]. The enhanced wedge-lok expands against both the card and the chassis, providing two or more heat transfer pathways, which improves the joint thermal conductance [11, 12].

Figure 5 (b) shows the test setup for thermal conductance characterization of the card retainers. Thermal conductance was calculated based on the temperature drop between the card edge 'D' and the average rail temperature 'J'. The average rail temperature was the average of temperatures measured at A, B, and C, and the card temperature was measured at 'D'.

Figure 5 (c) shows the thermal conductance comparison of the card retainers. Thermal conductance improved and plateaued as the applied torque increased. Improvement in thermal conductance with the enhanced wedge-lok was almost 233% at torque of 12 lbs-in (~1.36 N-m). Previously, these enhanced wedge-loks have demonstrated 150% better joint thermal conductance than conventional devices with the same form factor [10]. The reduction in thermal resistance can lower circuit card temperatures by 1-2°C, which can in turn increase component mean time between failure.

Performance of Electronics Cooling System

A system level assessment of the electronics cooling system was performed by testing both EHP and PHP heat spreader prototypes in a representative chassis enclosure using the enhanced wedge-lok. The size of the heat spreaders was 143mm x 146mm x 3.1mm. A 50mm x 50mm polyimide film heater was attached to the heat spreader to simulate a heat source. Heat was removed by circulating fluid through the cold plate chassis. Further details on the test setup can be found in [13].

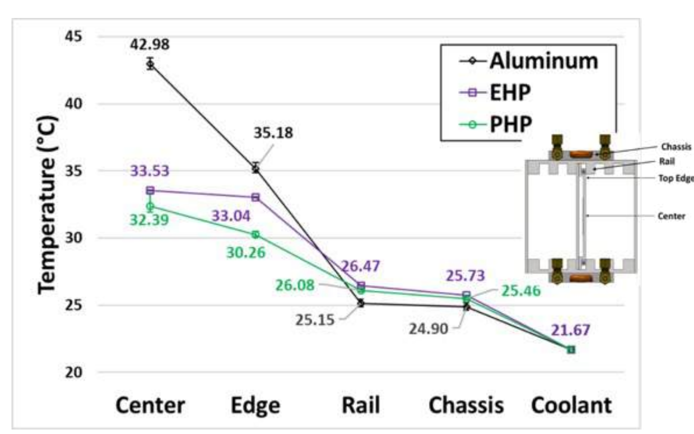

Fig. 6. - Instantaneous temperature profile of the electronics cooling system. Applied heater power was 21 W [13]. The temperature measurements at different locations of interest in the system is denoted in the schematic.

Figure 6 shows steady state temperature profiles of the electronics cooling system using different heat spreaders: aluminum plate (conventional), EHP and PHP. The maximum temperature on the aluminum spreader was ~43°C, while the EHP and PHP reduced the maximum temperature by 9.5°C and 10.6°C, respectively. In the EHP, temperature spreading from the center to edge was better than with the PHP. But the temperature drop from the edge to the rail was higher with the EHP because the heat transfer through the stepped plane was augmented by the fluid channels.

In the EHP, heat flows through the stepped plane only by material conduction. Overall, the EHP- and PHP-based cooling system showed very similar performance with approximately twice the thermal conductance relative to the baseline (i.e. aluminum plate) cooling system.

Conclusions

Thermal management of modern electronics dissipating large heat fluxes will require employing advanced cooling systems compared to the conventional technologies, such as aluminum conduction plate heat spreaders and conventional wedge-loks. Two forms of advanced heat spreaders: Embedded Heat Pipe (EHP) and Pulsating Heat Pipe (PHP) were presented as superior heat spreaders compared to aluminum spreaders. In general, the EHP works with significantly higher thermal conductance compared to an aluminum conduction plate at or above room temperature. In contrast, PHP had high thermal conductance at lower temperatures and heat fluxes. An enhanced wedge-lok card retainer, capable of expanding in two-directions and providing more heat transfer surface area, was shown to improve joint thermal conductance compared to conventional wedge-loks. At a system level, these technologies together can improve the thermal conductance and reduce the maximum temperature on the chips. This can improve the mean time between failure (MTBF) of future electronics and provide significant performance and cost benefits.

References

[1] https://www.1-act.com/products/hik-plates/

[2] S. D. Garner, "Heat Pipes for Electronics Cooling Applications," Electronics Cooling 2, 18-23, 1996

[3] R. Graham, "Heat Pipes," Thermopedia: Begel House, Inc., 2011

[4] https://www.1-act.com/resources/heat-pipe-calculator/

[5] S. Khandekar, M. Groll and V. Luckchoura, "An introduction to pulsating heat pipes," Electronics Cooling 9, 38-42, 2003

[6] J. Kim and S. J. Kim, "Experimental investigation on working fluid selection in a micro pulsating heat pipe," Energy Conversion and Management, 205, p. 112462, 2020

[7] B. L. Drolen and C. D. Smoot, "Performance Limits of Oscillating Heat Pipes: Theory and Validation," Journal of Thermophysics and Heat Transfer, 3 (4), 920-936, 2017

[8] B. S. Taft, A. D. Williams and B. L. Drolen, "Working Fluid Selection for Pulsating Heat Pipe," in AIAA Thermophysics Conference, Honolulu, Hawaii, 2011

[9] S. K. Hota, K. L. Lee, G. Hoeschele, R. Bonner and S. Rokkam, "Experimental Comparison on Thermal Performance of Pulsating Heat Pipe and Embedded Heat Pipe Heat Spreaders," in 2023 39th Semiconductor Thernal Measurement, Modeling & Management Symposium (SEMI-THERM), 2023

[10] https://www.1-act.com/products/ice-lok-thermally-enhanced-wedgelock/

[11] M. D. Flannery, J. Schmidt, J. Weyant and K. Thorson, "Thermal Enhancements for Separable Thermal Mechanical Interfaces," in AIAA: Spacecraft Thermal Management, 2016

[12] A. Slippey, W. G. Anderson, M. C. Ellis, C. Hose, J. Schmidt and J. Weyant, "Thermal Management Technologies for Embedded Cooling Applications," in 17th IEEE Intersociety Conference on Thermal and Thermomechanical Phenomena in Electronic Systems (ITherm) , 2018

[13] K. L. Lee, S. K. Hota, A. Lutz and S. Rokkam, "Advanced Two-Phase Cooling System for Modular Power Electronics," in 51st International Conference on Environmental Systems, St. Paul, MN, USA., 2022

[14] S. M. S. Murshed and C. A. N. de Castro, "A critical review of traditional and emerging techniques and fluids for electronics cooling," Renewable and Sustainable Energy Reviews, 78, 821-833, 2017

[15] C. Y. Tseng, H. M. Wu, S. C. Wong, K. S. Yang and C. C. Wang, "A Novel Thermal Module with 3-D Configuration Pulsating Heat Pipe for High-Flux Applications," Energies, 11 (12), 3425, 2018

[16] K. L. Lee, S. K. Hota and A. Lutz, "Advanced Cooling System for Modular Power Electronics," NASA SBIR Phase I Final Report (Distribution B) Contract#80NSSC21C0211, 2021

Rapid and Accurate Analytical Model for Predicting Axial Fan Performance in Electronics Cooling

Wenguang Zhao, Sahan Wasala, Tim Persoons
Department of Mechanical, Manufacturing and Biomedical Engineering, Trinity College Dublin, Ireland

Introduction

Forced air cooling remains essential for dissipating the heat generated by high-power-density devices in modern electronics [1]. Axial fans are widely used in information technology, telecommunications, automotive, and aerospace applications for air cooling. The aerodynamic performance (P-Q) curve of fans is essential for designing and optimising air-cooling systems. However, fan performance modelling can be challenging and is dependent on numerous factors that must be accurately accounted for. The lumped fan (LF) model is a well-established practise for modelling electronic enclosures with forced convection cooling by simplifying fan geometries as a plane. However, this makes it difficult to precisely predict swirl velocity profile and fan performance, leading to some margin of error in thermal-flow designs [2]. Although higher fidelity three-dimensional computational fluid dynamics (CFD) methods, such as the steady/unsteady Reynolds-averaged Navier-Stokes approach (U/RANS) and large eddy simulation (LES), have been proven more reliable in modelling fan performance, the high computing resource demand limits their use in rapid industrial design and optimisation cycles [3].

This study aims to develop and validate an analytical model for the fast and accurate prediction of the aerodynamic performance (*P-Q*) curve of axial cooling fans, accounting for actual fan geometry and the tip clearance effect. This prediction tool is anticipated to be highly appropriate for rapid design, analysis and optimisation of electronics cooling fans and enclosures, thereby facilitating future co-design of thermal-flow and noise.

Wenguang Zhao
Wenguang Zhao is a Ph.D. candidate in Mechanical Engineering at Trinity College Dublin, under the supervision of Dr. Persoons. He is a research student in the NSF Cooling Technologies Research Center at Purdue University. He received his B.E. degree in Thermal Energy and Power Engineering from Southeast University in China in 2017, followed by a M.E. degree in Power Engineering and Engineering Thermophysics from the same institution in 2020. His research interests are primarily focused on the aerodynamic and aeroacoustic modelling, optimisation techniques, and noise control strategies for electronics cooling.

Sahan Wasala
Sahan Wasala is a Visiting Research Fellow in the Department of Mechanical, Manufacturing & Biomedical Engineering at Trinity College Dublin. He was a SFI Research Fellow at CONNECT centre and a SFI RD&I Research Fellow at Seagate Technology LLC, USA. He received his Doctorate in Engineering Science at the University of Auckland, New Zealand. His research interests are focused on aerodynamic & aeroacoustics noise modelling and acoustic noise reduction methods, particularly using acoustic metamaterials. His present address is Applied Research and Technology, Collins Aerospace, Cork, Ireland.

Tim Persoons
Tim Persoons is Associate Professor in the Department of Mechanical, Manufacturing & Biomedical Engineering at Trinity College Dublin, and a visiting Faculty in the NSF Cooling Technologies Research Center at Purdue University. He received his Doctorate in Engineering from KULeuven in 2006. Dr. Persoons' research activities include multi-scale convective heat transfer and fluid dynamics for electronics thermal management and related thermo-fluid applications. He has authored over 150 journal and conference publications, serves in editorial roles for IEEE Trans Compon Packag Manuf Technol, Exp Therm Fluid Sci, ITherm, Therminic, Eurotherm, and was co-recipient of the 2013 Hartnett-Irvine Award and the 2020 Harvey Rosten Award.

Analytical Model

An analytical model for predicting the aerodynamic performance of fans was previously introduced by the authors in [4], [5]. This quasi-3D method was developed based on the lifting line theory, combined with blade element theory (BET) and the viscous vortex panel solver XFOIL [6]. The method is parametric and utilizes the actual blade geometry while accounting for tip loss. It assumes minimal radial flow, which allows the fan blades to be considered as a series of 2D radial elements. The shroud improves fan performance by suppressing tip vortices, and the method treats this suppression as an increase in sectional lift coefficients. The key equations of the analytical model are presented in this section and it was implemented in MATLAB.

Figure 1 illustrates the velocity triangles of a typical fan element. In practical applications, downstream stationary objects, such as streamlined stators/guide vanes or non-streamlined struts, are often present. This study models the downstream structure as an ideal stator with an imaginary shape that can fully recover the pressure loss due to the rotational velocity component, which is equal to $\rho v_u^2/2$.

The thrust dT and torque dM for a radial element dr can be expressed as:

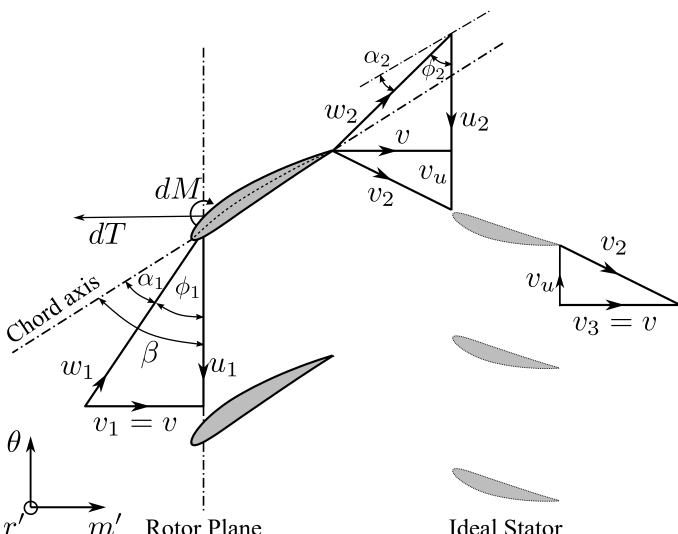

Fig. 1. Velocity triangles in fan blade elements and the ideal stator assumption.

$$dT = \frac{1}{2}\rho B \frac{\Omega^2 r^2 (1-a')^2}{\cos^2\phi} c(C_l \cos\phi - C_d \sin\phi) dr, \quad (1)$$

$$dM = \frac{1}{2}\rho B \frac{\Omega^2 r^2 (1-a')^2}{\cos^2\phi} c(C_l \sin\phi + C_d \cos\phi) r dr, \quad (2)$$

where C_l, C_d are the lift coefficient and the drag coefficient, respectively. r, Ω, B and c denote the blade radius, rotational speed, number of blades and chord length, respectively. ϕ is the effective inflow angle with respect to the rotor plane, which can be determined as:

$$\phi = \frac{1}{2}(\cot\phi_1 + \cot\phi_2), \quad (3)$$

where ϕ_1 and ϕ_2 are the inflow angle at inlet and outlet, respectively.

α' is the tangential induction velocity factor ($u = \Omega r\ (1 - \alpha')$), which can be expressed asned as:

$$a' = \frac{w_1}{\Omega r} \sin\phi \tan\alpha_i, \quad (4)$$

where w_1 is the total relative velocity at the blade leading edge ($w_1 = \sqrt{(u_1^2 + v_1^2)}$).

The root and tip loss for a finite-span blade were accounted for by assuming an elliptical lift distribution along the span. Based on the lifting line theory, the induced angle of attack α_i can be determined as:

$$\alpha_i = \alpha_1 - \alpha = \frac{C_l}{\pi AR_{eff}}. \quad (5)$$

where α denotes the effective angle of attack ($\alpha = \beta - \phi$).

The downwash resulting from the tip vortices exerts a diminishing effect on the lift coefficient slope of an airfoil with an infinite span. Therefore, the finite airfoil lift coefficient C_l is expressed as:

$$C_l(\alpha) = \frac{C_{l,\infty}(\alpha)}{1 + \frac{m}{\pi AR_{eff}}}, \quad (6)$$

where $C_{l,\infty}$ is the lift coefficient of a 2D airfoil with infinite span, obtained by XFOIL [6]. m is the slope of $C_{l,\infty}$ with respect to α. Lift and drag coefficients are calculated by polynomial interpolation from a pre-computed table, based on α. To ensure numerical stability, all aerodynamic data were computed using XFOIL in the range of -20º to +20º, extended to ±180º with the Viterna method [7]. XFOIL uses the e^n method to predict laminar-to-turbulent flow transition [6]. The paramete N_{crit}=5 was utilised to represent relatively high turbulence inflows.

By substituting *Equation 5* with *Equation 6*, and solving iteratively, the effective angle of attack α for each blade element can be determined. Then the forces and velocities can be obtained by solving *Equation (1) - (4)*.
The static to total pressure can be determined as:

$$P = \Delta P_t - P_d = \frac{T}{A} - \frac{1}{2}\rho v^2, \tag{7}$$

where, T is the total thrust of the rotor. A is the fan area.

This method considers the impact of tip clearance on fan performance using the effective aspect ratio AR_{eff}, which incorporates the correction factor M_{AR} with the geometric aspect ratio AR. A shroud can mitigate tip vortices and improve blade performance, but its effectiveness decreases with increasing tip clearance. To account for this, the tip clearance effect is modelled as an increase in M_{AR}, , and a linear correlation equation has been developed to select the appropriate value of M_{AR}, which can be expressed as:

$$M_{AR} = 1 + \max\left(0, 4.86\left(1 - \frac{T_R}{9.94}\right)\right). \tag{8}$$

Equation 8 is an empirical equation based on several CFD studies and experiments, which is recently developed in [8]. T_R is the tip clearance ratio, which is defined as $T_R=t/R_t$, and has a valid range from 0% to 10%. t and R_t denote the tip-gap width and the blade tip radius.

The theoretical fan performance based on Euler's work equation can be used for comparison with the developed method [9]. Assuming flow alignment with the geometrical camber line and ideal stator recovery of downstream pressure loss, the ideal static to total pressure can be expressed as [8]:

$$P_{ideal} = \Delta P_t - P_d = \rho u v_u - \frac{1}{2}\rho v^2, \tag{9}$$

where $v_u=u-v\cot\phi_2$. ϕ_2 can be approximated as the angle between the tangent of the camber line at the trailing edge and rotor plane.

Experimental Setup

To experimentally validate the proposed fan model, a wind tunnel was developed based on ANSI/AMCA 210-16 [9], as shown in *Figure 2*. A modification was made to the setup by using a standardised orifice plate, in accordance with ISO 5167-2:2003 [10], to measure airflow rates. This method provides high accuracy and is easier to implement than the Pitot tube method used in the original AMCA standard. A honeycomb flow straightener is used to rectify non-axial airflow, and a throttling device at the end of the tunnel enables control of the fan backpressure. Due to the presence of system resistance inside the tunnel, the static pressure around the fan outlet cannot reach the free delivery condition (zero backpressure). In this case, an auxiliary fan could be added as an exhaust system. The total volumetric flow rate, Q, and the static-to-total pressure rise across the test fan, P, can be obtained following the ANSI/AMCA standardized procedures [10].

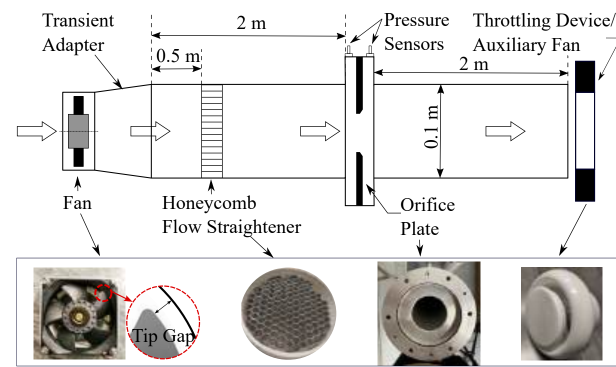

Fig. 2. Experimental setup for testing fan aerodynamic performance according to ANSI / AMCA 210-16 [10] and ISO 5167-2:2003 [11].

Case Study

An 80 mm diameter cooling fan with 5 blades and a blade tip clearance ratio of 2.5% was selected to validate the aerodynamic model. The fan, which operates at 9000 RPM, is used in a commercial multiple hard disk drive enclosure and has been previously studied in [4], [5]. The blade tip radius and hub radius are 37.35 mm and 18.7 mm, respectively, while the tip Mach number is approximately 0.1 and the averaged chord-based tip Reynolds number is around 60,000.

The blade was divided into sections and twist and chord distributions were extracted from a CAD file (see *Figure 3*). Airfoil profile coordinates were non-dimensionalized to calculate aerodynamic coefficients. In cases where CAD files are unavailable, 3D scanning can be used to extract blade information. If none of these options is available, airfoil databases such as [12] may be used to find a similar airfoil based on maximum camber and thickness measurements. For the test case, the mid-span airfoil profile had a maximum thickness of 6.7% at 23.6% chord and a maximum camber of 2.2% at 49.0% chord. This information aided in identifying similar airfoils in [12], specifically AG26 and AG17, which were selected to assess the model's sensitivity to airfoil coordinates.

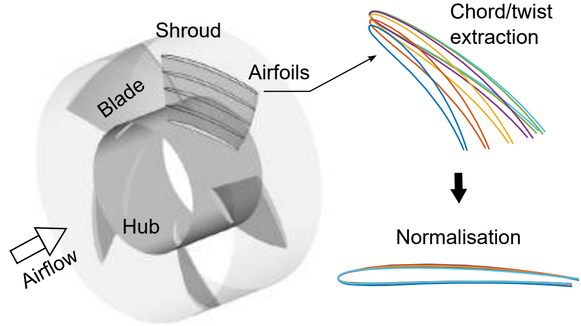

Fig. 3. A schematic for extracting fan design parameters from CAD or 3D-scanned files.

To determine the optimal aspect ratio correction factor M_{AR}, *Equation 8* was employed with a tip clearance ratio of $T_R = 2.5\%$, resulting in a value of 4.6. The fan performance curve (*P*-*Q*) was calculated using the analytical model outlined in Section II.

Figure 4 shows the predicted *P*-*Q* curves with the optimal correction factor ($M_{AR} = 4.6$) using the three similar airfoil profiles, compared to the reference data provided by the manufacturer and experimental data. Reasonable agreement is observed between the predicted results using the real fan airfoil profile and the experimental data, except for some discrepancies near and after the stalling dip, as shown in *Figure 4*. The normalized root-mean-square error (NRMSE) is 5.0% in the nominal working region, while it increases to 13.0% in the stall region. The flow becomes unstable and separates in the stall region, increasing the radial flow component, causing the axial fan to behave like a mixed-flow fan [13] and invalidating the zero-radial flow assumption. Although this XFOIL [6] based model can partially predict near-stall and post-stall fan performance, it is less accurate in the stall region due to the absence of radial flow consideration. Moreover, *Figure 4* demonstrates that using similar airfoil profiles (AG26 and AG17) in this method can provide comparable predictions except for the stalling dip region, which appropriately relaxes the minimum requirement of this model for airfoil profile data.

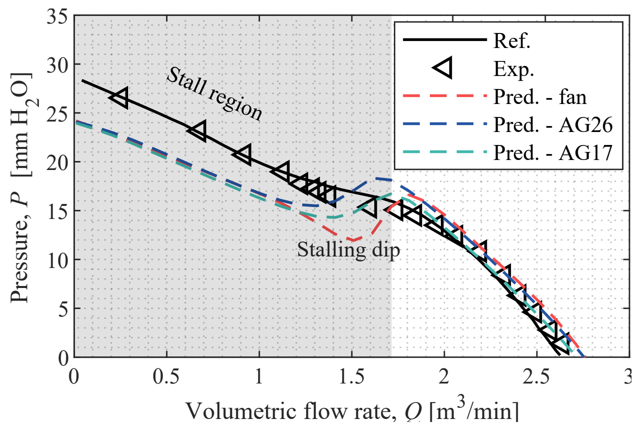

Fig. 4. Comparative analysis of fan performance using multiple airfoil coordinates: reference, experiment, and prediction with correction factor M_{AR}=4.6.

To further investigate the influence of airfoil characteristics on the prediction of the fan PQ curve, various NACA 4-digit airfoil profiles were employed. NACA 4-digit is a system for airfoil designations developed by NACA. It uses a four-digit number to describe an airfoil's shape and characteristics, including maximum camber, camber position, and thickness-to-chord ratio. To represent the original fan profile, a NACA 2507 was used as a baseline case, having 2% maximum camber, positioned 50% from the leading edge, and a 7% thickness-to-chord ratio. Additionally, NACA 2503 and NACA 2515 airfoils were chosen to investigate the impact of airfoil thickness, while NACA 0507 and NACA 6507 airfoils were employed to examine the effect of airfoil camber. Figure 5 illustrates the results, showing that airfoil thickness primarily influences the onset of the stall region, while exerting minimal impact on the low-pressure region. On the other hand, airfoil camber plays a more significant role in the prediction of the PQ-curve, as it can modify the zero-lift angle of attack and affect the overall performance of the fan.

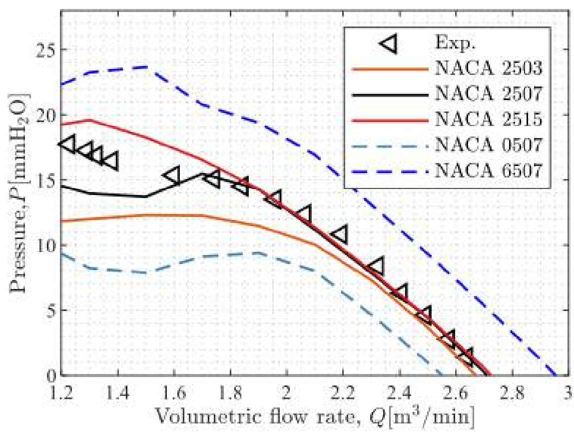

Fig. 5. Effect of the airfoil thickness and camber on fan performance prediction.

Figure 6 epicts the impact of effective aspect ratio correction factor on predicted P-Q curves for different M_{AR} values ($1 \leq M_{AR}, \leq \infty$) in comparison to the reference, experimental, and ideal curves. Generally, an increasing M_{AR} value leads to higher predicted fan performance. Specifically, $M_{AR} = 1$ indicates a fan with finite span and large tip clearance, while $M_{AR} \rightarrow \infty$ approximates an ideal fan curve for a fan with infinite span and zero tip clearance. The proposed aspect ratio correction factor, M_{AR}, ddemonstrates promising analytical capabilities in accounting for finite span and tip clearance effects in predicting fan curves.

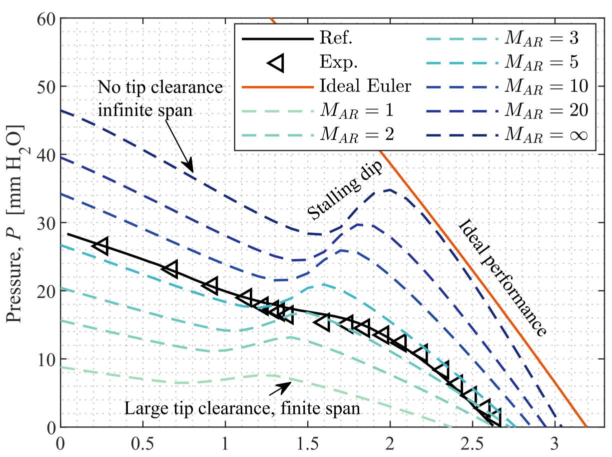

Fig. 6. Effect of the correction factor M_{AR} on fan performance prediction.

The proposed aerodynamic model can be seamlessly integrated with an aeroacoustic model to predict far-field noise levels. More details on this aeroacoustic model can be found in [4] [5].

The combined model takes approximately 10 minutes on an Intel Xeon E5-2630v3 CPU utilizing 8 cores (1.3 core-hours), which is more than three orders of magnitude faster than the high-fidelity method (9,600 core-hours) in [3].

Conclusion

In this study, an analytical model was presented to analyse the aerodynamic performance of electronic cooling fans in a computationally efficient and accurate manner. The model accounts for the actual fan geometry and the impact of tip clearance. This model was validated against experimental tests conducted on a standardized test facility, yielding a prediction error within 5% in the fan's nominal working conditions. Overall, the proposed analytical model can reasonably predict fan performance with an ultra-low computational cost. This model could be beneficial in accelerating and optimizing the thermal-flow design of fan-cooled electronics systems, while also offering valuable insight into future noise control.

References

[1] [1] S. V. Garimella, T. Persoons, J. A. Weibel, and V. Gektin, "Electronics thermal management in information and communications technologies: challenges and future directions," IEEE Transactions on Components, Packaging and Manufacturing Technology, vol. 7, no. 8, pp. 1191–1205, Aug. 2017.

[2] G. V. Shankaran and M. B. Dogruoz, "Validation of an advanced fan model with multiple reference frame approach," in 2010 12th IEEE Intersociety Conference on Thermal and Thermomechanical Phenomena in Electronic Systems. Las Vegas, NV, USA: IEEE, Jun. 2010, pp. 1–9.

[3] S. Wasala, Y. Xue, T. Wiegandt, L. Stevens, and T. Persoons, "Aeroacoustic noise prediction from a contra-rotating cooling fan used in data center cooling systems," in AIAA AVIATION 2021 FORUM. AIAA Paper 2021-2313, 2021. [Online]. Available: https://arc.aiaa.org/doi/10.2514/6.2021-2313

[4] W. Zhao, S. Wasala, and T. Persoons, "Reduced-order aeroacoustic modeling of electronics cooling fans," in 28th International Congress on Sound and Vibration, Singapore, 2022. [Online]. Available: https://iiav.org/content/archives_icsv_last/2022_icsv28/content/papers/papers/full_paper_91_20220418214546788.pdf

[5] W. Zhao, S. Wasala and T. Persoons, "Towards quieter air-cooling systems: Rotor self-noise prediction for axial cooling fans," in 28th International Workshop on Thermal Investigations of ICs and Systems (THERMINIC). IEEE, Sep 2022, pp. 1–4. [Online]. Available: https://ieeexplore.ieee.org/document/9950669/

[6] M. Drela, "XFOIL: An analysis and design system for low Reynolds number airfoils," in Low reynolds number aerodynamics, T. J. Mueller, Ed. Berlin, Heidelberg: Springer Berlin Heidelberg, 1989, pp. 1–12.

[7] R. D. Viterna, L. A., Corrigan, "Fixed pitch rotor performance of large horizontal axis wind turbines," in NASA Lewis Research Center: Energy Production and Conversion Workshop. NASA Lewis Research Center Cleveland, OH, United States, 1982. [Online]. Available: https://ntrs.nasa.gov/citations/19830010962

[8] W. Zhao, S. Wasala, T. Persoons, On the fast prediction of the aerodynamic performance of electronics cooling fans considering the effect of tip clearance, IEEE Trans Compon Packag Manuf Technol (in review, Apr 2023).

[9] W. T. W. Cory, Fans & ventilation: a practical guide. Amsterdam; Boston: Elsevier in association with Roles & Assoc, 2005.

[10] AMCA - The International Authority on Air System Components, "ANSI/AMCA Standard 210-16/ASHRAE Standard 51-16 - Laboratory methods of testing fans for certified aerodynamic performance rating," 2016. [Online]. Available: www.amca.orgwww.amca.org/store.

[11] International Organization for Standardization, "ISO 5167-2:2003 Measurement of fluid flow by means of pressure differential devices inserted in circular cross-section conduits running full — Part 2: Orifice plates," 2003.

[12] "Airfoil tools," [Online]. Available: http://airfoiltools.com/, Mar. 2023.

[13] F. P. Bleier, Fan handbook: selection, application, and design. New York: McGraw-Hill, 1998.

A Comparative Summary of Data Center Cooling Strategies

Dr. Tim Shedd
Engineering Technologist with the CTO's Office
Dell Technologies

Dr. Emily B. Clark
Thermal Technologist in the Chief Technology Office
Dell Technologies

Introduction

Industry power trends and a global push for sustainability are leading decision makers and data center operations groups to consider alternatives to traditional air cooling. Two key industry trends are driving alternative cooling solutions. First, powers at the chip level are increasing [1,2]. Just a couple of years ago, server CPU and GPU power levels were only 205 W and 300 W, respectively. Today, performance competition among CPU vendors is pushing power towards 500 W. Artificial intelligence and machine learning workloads have pushed GPU power to 700 W with 1000 W likely just around the corner. Increased CPU and GPU power impacts the temperatures at which these components can operate. The silicon that makes up these parts is temperature limited. Because of the silicon limits, the junction temperature can be considered fixed. When more power is pushed through the processor package, the case temperature must come down to keep the junction temperature the same to maintain operationality. On the one hand, the powers are increasing higher and higher, while on the other, the CPUs and GPUs must be cooled to lower and lower temperatures [1,3]. This stresses the traditional air-cooling approach, which is leading to consideration of new liquid cooling solutions [4,5,6,7]. In addition to the power and temperature trends, the global energy crisis is pushing all sectors to be more sustainable. For servers and data centers, this sustainability push means operators are targeting green energy sources, overall reductions in facility energy use, and the reduction or elimination of water use. These industry challenges require new cooling solutions to both enable sufficient cooling at power levels beyond the capability of air cooling and to yield solutions that offer realizable sustainability opportunities. Five unique cooling solutions exist in the market today; each have varying cooling performance, cost, and reliance on facility chilled water supplies. These technologies include: air cooling using larger server chassis form factors, direct liquid cooling (DLC) using water or Propylene Glycol (PG) solutions, DLC using two-phase dielectric fluids, single phase immersion, and two-phase immersion. The thermal performance of these technologies was compared using simplified, algebraic thermal models. The full work has been published in the IEEE Proceedings of SEMI-THERM 39 [8]. This work focuses on the thermal solution alone, which is only one of the factors considered when selecting a cooling technology. In picking a cooling solution, one should also consider the relative cost, complexity, serviceability, and environmental impact of each technology in addition to data center facilities and the relative thermal performance of the cooling solutions.

Dr. Emily Clark
Dr. Emily Clark is a Thermal Technologist in the Chief Technology Office at Dell Technologies. She focuses on thermal solutions and innovations for server and data center cooling. Emily completed her PhD as a Bredesen Center Fellow at the University of Tennessee. She performed her doctoral research at Oak Ridge National Laboratory, which focused on cooling of plasma-facing components in nuclear fusion reactors. She previously worked at Raytheon Technologies, where she focused on cooling complex systems.

Dr. Tim Shedd
Dr. Tim Shedd is currently an Engineering Technologist with the CTO's office of Dell Technologies, where he provides thermal strategy, product innovation and business development for Dell's data center products. Prior to this, he was the Director of Research and Development at Motivair Corporation, preceded by a role as the Director of Product Management for Zutacore, Inc. From 2013 to 2017, Shedd led a startup company, Ebullient, Inc., to commercialize a novel, scalable electronics cooling technology that was initially conceived while a faculty member at the University of Wisconsin-Madison. He holds multiple patents issued for direct liquid cooling technologies and low-emissions carburetors. He is a fellow of the American Society of Heating, Refrigeration and Air-conditioning Engineers (ASHRAE) where he chairs the SSPC 127 Subcommittee developing standards for the Methods of Test for Data Center Liquid Cooling Equipment.

Figure 1 shows a simplified data center and its end-to-end thermal management system. The system was broken down into three components: heat collection (blue), heat transport (grey), and heat rejection (green). In the heat collection portion, the cooling technology captures the heat from the IT gear. For transport, the heat is carried from the technology cooling system to the heat rejection system. Lastly, the heat rejection segment generates relatively cool facility water by rejecting the heat to the local environment. If an air-cooled system is taken as an example, then heat collection occurs as the air blows past finned heat sinks and circulates to the air handler. Facility water then removes the heat from the air and the heat is rejected to the ambient environment.

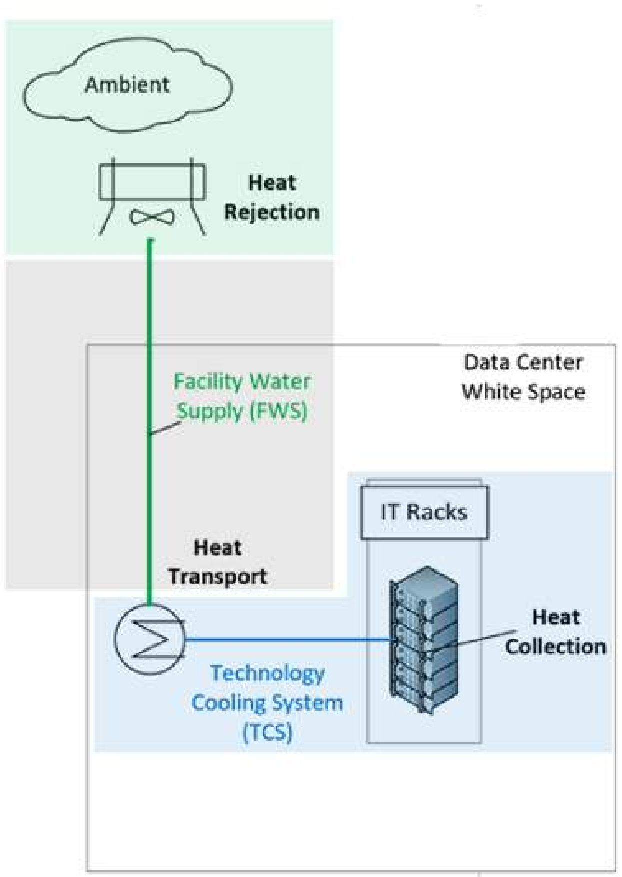

Fig. 1. Simplified end-to-end data center thermal management diagram.

Unique cooling solutions in the market each have different performance, cost, and facility water requirements. Six configurations were represented as simplified thermal models for this comparison:

- Air-cooling in a 1U configuration
- Air-cooling in a 2U configuration
- Single-phase DLC (1-2 liters per minute, lpm)
- Two-phase DLC
- Single-phase immersion
- Two-phase immersion

Figure 2 represents the simplified thermal model for air-cooled servers. The heat collection portion of the end-to-end system was broken down into two primary thermal resistances: one at the server level (orange) and another at the facility level (blue). The server level captures the resistance between the chip case and the air (θc,a), while the facility level, i.e. computer room air handler (CRAH) represents the resistance between the air and the facility water ($\theta_{a,FWS}$). The resistance at the server level was modeled from experimental data and the resistance on the facility side was gathered from manufacturers' data. Both air-cooled configurations (1U and 2U) are represented by *Figure 2.* The primary difference in the model for these configurations is the heat sink resistance value, which can be viewed in *Reference 8.* Furthermore, *Reference 8* provides simplified thermal models and corresponding resistance values for the remaining cooling technologies, including immersion and DLC.

When reviewing the results of the thermal modeling, it is important to keep in mind the following about the thermal resistances used:

1) These values represent typical server thermal resistances for an Intel Sapphire Rapids Thermal Test Vehicle (TTV) used according to Intel's specifications. Data for the same TTV design was used for all of the thermal technologies, allowing for an apples-to-apples comparison.

2) The heat sinks, cold plates, etc. tested were typical for the generation of servers launched in early 2023. There are devices across the technologies that can achieve higher performance. There may be higher performing TIM materials. However, the intent was to compare devices that are deployed at scale, or could be deployed at scale, and thus considerations must be made for quality, reliability and scalability of the thermal technology devices.

3) Even with the above considerations, data center servers have wide-ranging designs and no two deployments are identical. This study intentionally ignored important behaviors like pre-heating of coolant from other components in the server so that we could focus on a direct comparison of the thermal technologies in a truly one-to-one manner. Actual thermal resistance performance in the field can be expected to vary by up to 20% for a given thermal technology.

4) The temperatures shown in *Figures 4 and 5* should be used only to compare technologies and not as design recommendations. Again, this study intentionally simplified the cooling systems so that the performance of different cooling technologies could be compared. The actual cooling water temperatures will certainly vary depending on the exact deployment. Keep in mind that in most cases, the cooling water temperatures shown will tend to be optimistic, i.e., higher, compared with actual data center deployments.

5) The authors are aware of improvements being made in the areas of air-cooled heat sinks and closed loop Liquid Assisted Air Cooled (LAAC) systems since the testing for this study was per-

formed. Single-phase immersion systems are expected to improve similarly. While this will extend the range of processors that these technologies can cool, these improvements do not significantly impact the conclusions of the relative performance of the technologies, nor the general trend toward the need for liquid cooling as processor TDPs increase. Nor do we see indications that single phase immersion thermal resistances will vary significantly from air-cooled heat sink thermal resistances.

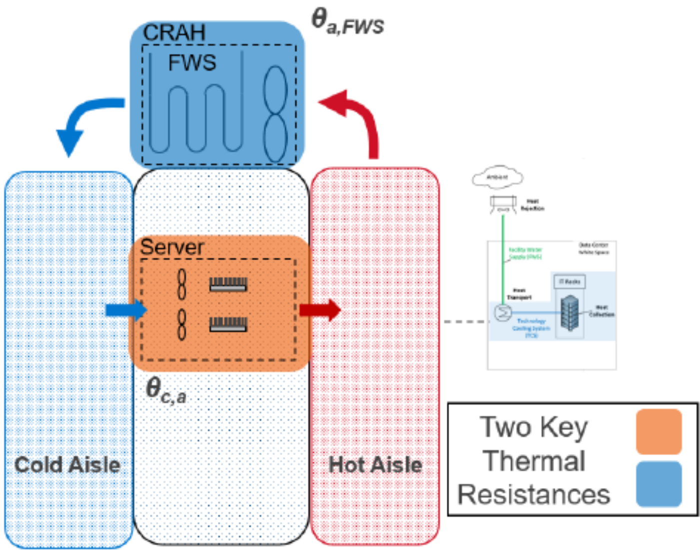

Fig. 2. Simplified thermal model for air-cooling.

We can visualize how the thermal resistance affects the maximum theoretical facility water (FWS) temperature for each of the technologies with a thermal stack-up chart. *Figure 3* shows an example of the thermal stack-up for air-cooling in a 2U configuration; this includes a 32-server rack with dual 250W processors. For 250W processors, we assume a maximum processor case temperature of 80°C, as indicated by the red dashed line. The orange bar represents the temperature difference due to the server level thermal resistance between the processor case and the air (θc,a). In this example, the case-to-air resistance leads to a temperature difference of about 20°C. The blue bar represents the temperature difference due to the facility side resistance ($\theta_{a,FWS}$), which is approximately 7°C. Taking the total temperature difference between the case and the facility water (27°C), and subtracting that from the maximum processor case temperature (80°C), gives the maximum allowable FWS temperature of 53°C.

Figure 4 shows the thermal stack-up for all technologies considered with 250W processors. The maximum FWS temperature for each technology can be compared against the W32 line in green on the chart. W32 is a liquid cooling class from the ASHRAE equipment environment specifications for liquid cooling, and it corresponds to 32°C facility water [9]. W32 is a useful reference because, in many climates, facility water can be maintained at this temperature with minimal use of compressors. Each technology has a reference point relating to the maximum processor case temperature except for two-phase immersion. Because two-phase immersion includes boiling at atmospheric pressure, the reference point for that technology must be the boiling point for the fluid, which is taken to be 50°C. For 250W processors, all the technologies investigated allow for FWS temperatures above 32°C. Two-phase immersion requires the lowest theoretical FWS temperature at 38°C. This is followed by air in a 1U configuration and single-phase immersion, which have similar maximum FWS temperatures. Air in a 2U configuration allows for slightly higher temperatures on the facility side, and single-phase and two-phase DLC allow for much higher FWS temperatures at this power level.

Figure 5 shows the impact of increasing the processor power to 500 W. For this power level, the maximum processor case temperature is reduced to 68°C, which is an estimate for future processors at this operating point. There is a notable difference in the maximum FWS temperatures. Air cooling in a 1U configuration and single-phase immersion are the most challenged by this higher power; their resistances lead to negative facility water temperature requirements. Furthermore, air in a 2U configuration and two-phase immersion both require FWS temperatures below W32. In contrast, single-phase and two-phase DLC still allow for FWS temperatures greater than W32 with plenty of headroom. Lastly, as the power increases from 250W to 500W per processor, the impact of the thermal resistance across the condenser for two-phase immersion and DLC greatly increases.

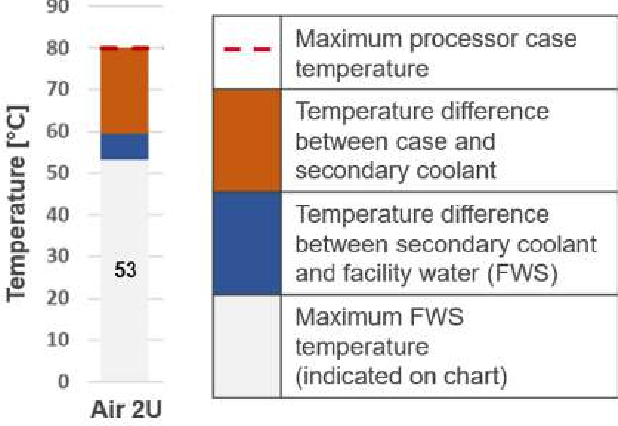

Fig. 3. Example of thermal stack-up for air-cooling in a 2U configuration.

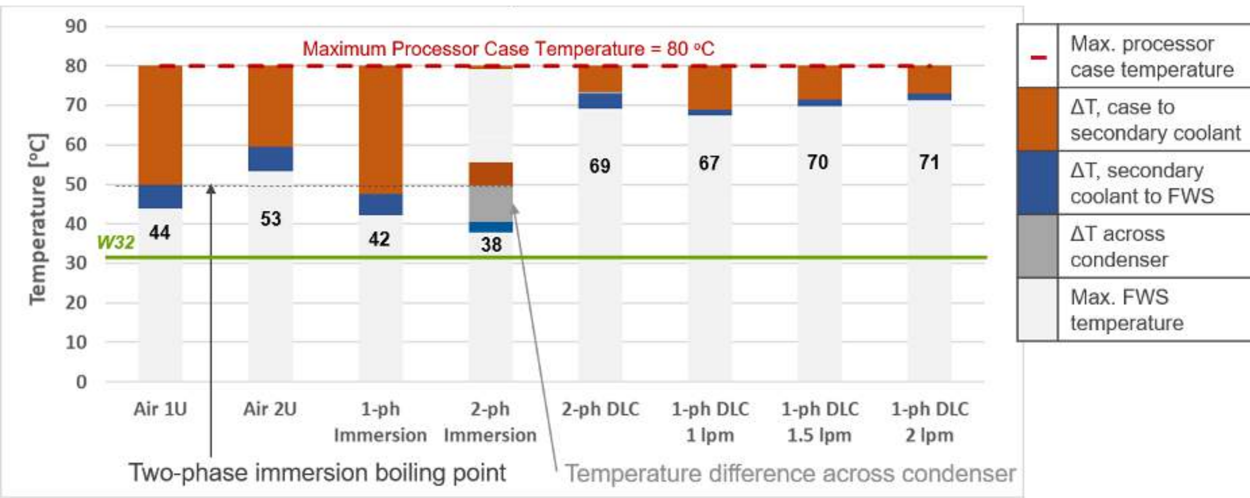

Fig. 4. Thermal stack-up comparison for 250 W processors.

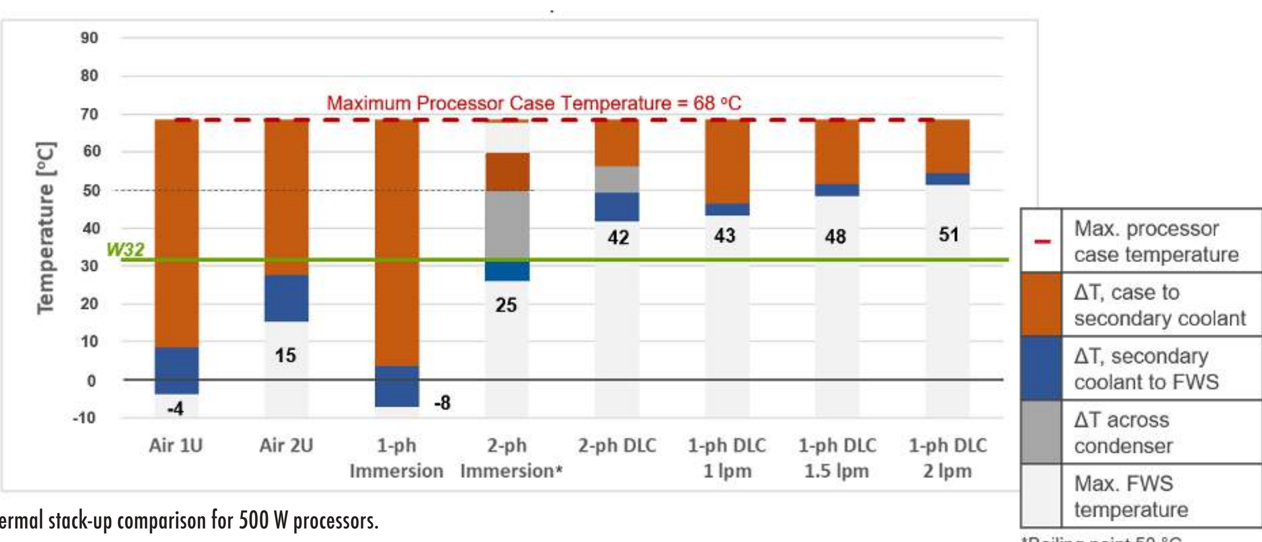

Fig. 5. Thermal stack-up comparison for 500 W processors.

The end-to-end temperature difference between the chip case and the facility water can also be visualized in a V-plot. *Figure 6* shows an example of the connection between the stack-up plots and the V-plots for air cooling in a 2U configuration. A box is drawn around the end-to-end temperature difference on the stack-up, as indicated by the blue arrow. This arrow is then added to the V-plot on the right. The left-hand guide represents increasing facility water temperatures, while the right-hand guide represents decreasing chip package temperatures. The end-to-end temperature difference is shown within the V created by these two guides. For this visualization, the thermal resistance decreases from top to bottom. A technology with a lower thermal resistance will be at the bottom of the chart, and a higher resistance will sit at the top.

Figure 7 shows the end-to-end temperature difference for all the technologies for 250W processors. Air cooling for a 1U configuration and single-phase immersion have similar thermal performances and have the highest thermal resistances. Single-phase and two-phase DLC are at the bottom of the chart with the lowest thermal resistances. Two-phase immersion and air cooling in a 2U configuration fall in the middle.

Figure 8 shows the comparison when the power is increased to 500W. There is a wider range in the end-to-end temperature difference, as shown by the increased spacing. Notably, because air cooling for a 1U configuration and single-phase immersion had temperature differences greater than 60°C, they are not shown on the plot. Single-phase DLC exhibits the lowest temperature difference and thus, the lowest thermal resistance. Two-phase DLC is close to single-phase DLC with 1 lpm, and two-phase immersion follows. Air cooling in a 2U configuration has a large temperature difference, indicating thermal challenges at this power.

Example: 2U Air Cooling

32 server rack of dual 250 W processors

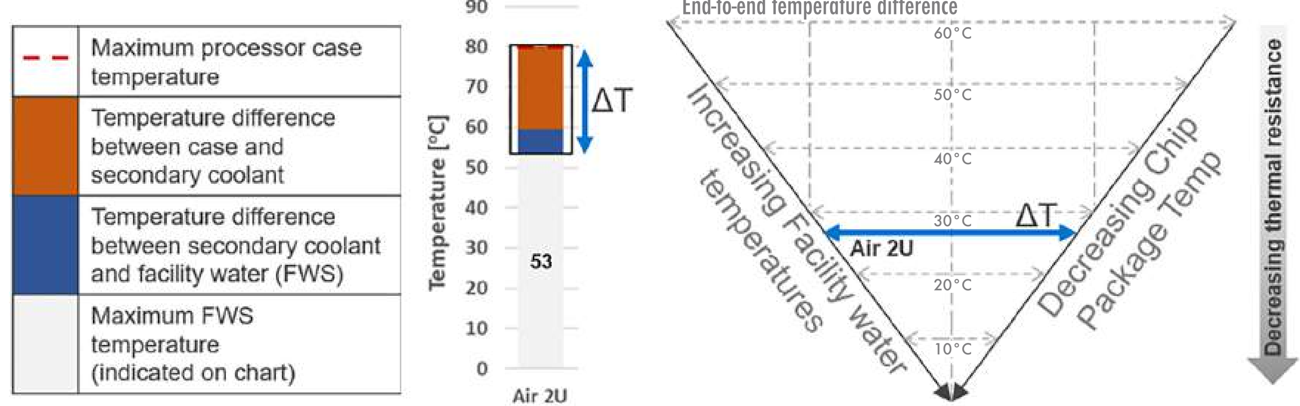

Fig. 6. Air-cooling example for visualizing end-to-end temperature difference.

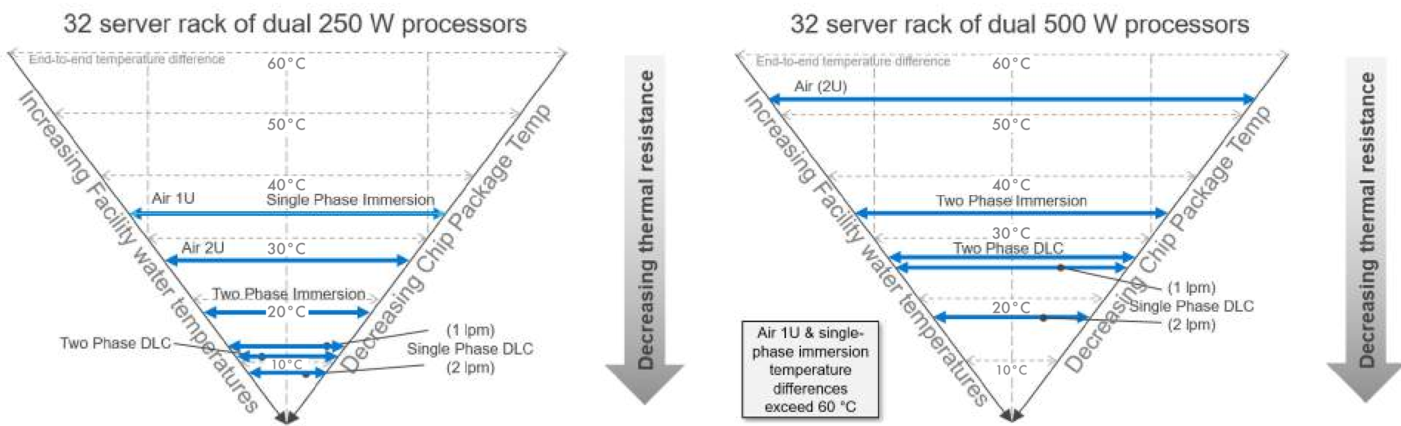

Fig. 7. End-to-end temperature difference for 250 W processors.

Fig. 8. End-to-end temperature difference for 500 W processors.

In comparing the thermal performance of different technologies, we see that air cooling and immersion cooling are challenged by high powers approaching 500 W and beyond. These limits may be pushed further by advances in heat sinks and air movers or circulators for air cooling and immersion, respectively. The limits could also be pushed further by larger processor footprints, which would spread the heat flux over a wider area. It should be noted that air cooling is often limited by the impact of the processor heat on the other components in the system. This impact was not included in the simplified thermal models, but it should be considered in a system design. The limiting factors for two-phase immersion are the fluid boiling points and the condenser performance. Single-phase and two-phase DLC were shown capable of cooling up to 500W processors with available thermal margin to W32 facility water. A limiting factor for two-phase DLC is the flow resistance of the vapor return path; this should be addressed in future design iterations. Advances in designs or fluids may improve two-phase DLC performance. Single-phase DLC was shown to have the best thermal performance of the technologies investigated with a potential to cool at least 1500W processors.

It is important to stress that this work focuses purely on the thermal performance of these different cooling technologies as they stand today, and it does not consider other important aspects in the selection of a cooling strategy such as relative cost, complexity, serviceability, and environmental impact of each technology. Based on this thermal performance analysis, while innovations are expected in each of the technologies, it appears that DLC will require the fewest technical improvements to meet future cooling needs.

References

[1] *Intel Product Specifications*, Intel Corporation, 2023, https://ark.intel.com/. Accessed 12 Jan. 2023.

[2] *AMD Product Resource Center*, Advanced Micro Devices, Inc.,2023, https://www.amd.com/en/products/specifications/. Accessed 12 Jan. 2023.

[3] "Thermal Design Guide for Socket SP3 Processors," *AMD Tech Docs*, Advanced Micro Devices, Inc., Publication number 55423, Rev. 3, Nov. 2017. Accessed Online. 2023, https://www.amd.com/en/support/tech-docs. Accessed 12 Jan. 2023.

[4] Kheirabadi, A. C., Groulx, D., "Cooling of server electronics: A design review of existing technology," *Applied Thermal Engineering*, Vol. 105, pp. 622-638, 2016[5] W. Zhao, S. Wasala and T. Persoons, "Towards quieter air-cooling systems: Rotor self-noise prediction for axial cooling fans," in 28th International Workshop on Thermal Investigations of ICs and Systems (THERMINIC). IEEE, Sep 2022, pp. 1–4. [Online]. Available: https://ieeexplore.ieee.org/document/9950669/

[5] Shahi, P., et al., "CFD analysis on liquid cooled cold plate using copper nanoparticles," ASME 2020 International Technical Conference and Exhibition on Packaging and Integration of Electronic and Photonic Microsystems, Virtual, 27-29 Oct., 2020.

[6] Shahi, P., Saini, S., Bansode, P., Agonafer, D., "A comparative study of energy savings in a liquid-cooled server by dynamic control of coolant flow rate at server level," *IEEE Transactions on Components, Packaging and Manufacturing Technology*, Vol. 11, No. 4, pp. 616-624, 2021.

[7] Fan, Y., Winkel, C., Kulkarni, D., Tian, W., "Analytical design methodology for liquid based cooling solution for high TDP CPUs," 2018 17th *IEEE Intersociety Conference on Thermal and Thermomechanical Phenomena in Electronic Systems (ITherm)*, 2018, pp. 582-586, doi: 10.1109/ITHERM.2018.8419562.

[8] Curtis, R., Shedd, T., and Clark, E.B., "Performance Comparison of Five Data Center Server Thermal Management Technologies," *2023 39th Semiconductor Thermal Measurement, Modeling & Management Symposium (SEMI-THERM)*, San Jose, CA, USA, 2023.

[9] *2021 Equipment Thermal Guidelines for Data Processing Environments: ASHRAE TC 9.9 Reference Card, ASHRAE, From Thermal Guidelines for Data Processing Environments*, Fifth Ed., 2021.

Call for Authors and Contributors!

Want to be a part of the next issue of Electronics Cooling? Have an article or blog post you'd like to write for Electronics-Cooling.com?

Let us know at
editor@electronics-cooling.com

www.Electronics-Cooling.com

Index of ADVERTISERS

cadence

t: (408) 943-1234
e: https://www.cadence.com/en_US/home/support.html
w: www.cadence.com
page: 5

Electronics Cooling

t: 484.688.0300
e: info@electronics-cooling.com
w: www.electronics-cooling.com
page: 33

LECTRIX

t: (484) 688-0300
e: info@lectrixgroup.com
w: www.lectrixgroup.com
page: 35

SIEMENS Digital Industries Software

t: (800) 592-2210
e: www.plm.automation.siemens.com/global/en/contact-us.html
w: www.plm.automation.siemens.com/global/en/
page: 2

Break the same old pattern.
Problem First. Product Last.
Content | Data | Marketing Technology
LECTRIX®
Digital Marketing for the B2B Electronics Industry
1.484.688.0300 | info@lectrixgroup.com
www.lectrixgroup.com